Acceleration of plague outbreaks in the second pandemic

David J. D. Earn[a,b,c,1], Junling Ma[d], Hendrik Poinar[b,c,e,f], Jonathan Dushoff[a,b,c], and Benjamin M. Bolker[a,b,c]

[a]Department of Mathematics & Statistics, McMaster University, Hamilton, ON L8S 4K1, Canada; [b]Department of Biology, McMaster University, Hamilton, ON L8S 4K1, Canada; [c]Michael G. deGroote Institute for Infectious Disease Research, McMaster University, Hamilton, ON L8S 4K1, Canada; [d]Department of Mathematics & Statistics, University of Victoria, Victoria, BC V8W 3R4, Canada; [e]McMaster Ancient DNA Centre, Department of Anthropology, McMaster University, Hamilton, ON L8S 4K1, Canada; and [f]Department of Biochemistry, McMaster University, Hamilton, ON L8S 4K1, Canada

Edited by Burton H. Singer, University of Florida, Gainesville, FL, and approved August 19, 2020 (received for review March 25, 2020)

Historical records reveal the temporal patterns of a sequence of plague epidemics in London, United Kingdom, from the 14th to 17th centuries. Analysis of these records shows that later epidemics spread significantly faster ("accelerated"). Between the Black Death of 1348 and the later epidemics that culminated with the Great Plague of 1665, we estimate that the epidemic growth rate increased fourfold. Currently available data do not provide enough information to infer the mode of plague transmission in any given epidemic; nevertheless, order-of-magnitude estimates of epidemic parameters suggest that the observed slow growth rates in the 14th century are inconsistent with direct (pneumonic) transmission. We discuss the potential roles of demographic and ecological factors, such as climate change or human or rat population density, in driving the observed acceleration.

plague | London | epidemic growth rate | reproduction number | COVID-19

Plague epidemics have afflicted human populations since at least the sixth century (1, 2). These events have had dramatic and long-lasting effects on human demography and behavior, especially those outbreaks associated with the second pandemic (14th to 19th centuries) in Europe and Asia (1, 3–5), and have inspired many theoretical studies of the ecology and evolution of infectious disease (6–13). We are now in the third pandemic (Modern Plague), with outbreaks continuing to occur in some parts of the world (14–18). Plague also remains a source of concern due to the bioterror potential of the causative agent, *Yersinia pestis* (19, 20).

Recent advances in paleogenomics have definitively established that historical plague pandemics were caused by *Y. pestis* (21, 22), as proposed in the 19th century after Yersin discovered the bacterium's link to bubonic plague (23). Researchers have reconstructed the evolutionary history of plague and other pathogens by sequencing and reconstructing nearly complete pathogen genomes from persistent DNA fragments (21, 24, 25). The strain isolated from victims of the Black Death (London 1348) is remarkably similar to extant human strains (Modern Plague): the core genomes* of these strains are $\approx 99.99\%$ similar (21), which makes it challenging to identify important evolutionary or ecological patterns from genomic investigations alone. Here we complement genetic studies by exploring more traditional (historical, demographic, and epidemiological) sources of information from a 300-y span of plague outbreaks in the same location (London), revealing a striking change in plague transmission dynamics over the course of the Renaissance period, namely, a fourfold increase in the initial growth rate of outbreaks.

We quantify this change without making any assumptions about the underlying transmission processes, exploiting methodology that we have developed previously for this purpose (26). We then consider how this inference can contribute to the debate concerning whether plague transmission was primarily indirect (via rat fleas) or direct (pneumonic human-to-human). We argue that strictly pneumonic transmission in the 14th century is implausible but that beyond this the best that can be done at present is to highlight the biological complexities and uncertainties that limit the potential for further inferences.

Data

The city of London, United Kingdom, is unusual in the extent to which patterns of death and disease can be reconstructed from extant documents. We have analyzed three sources of data (Fig. 1).

London Bills of Mortality. The London Bills of Mortality (LBoM) (27, 28) provide weekly counts of deaths by cause during each of the known plague epidemics in the 16th and 17th centuries. The LBoM thus give us information specifically about mortality attributable to plague for each epidemic, which we will use as a proxy for plague incidence (6, 26). When available, the LBoM are our most reliable records (except for the epidemic of 1593; *SI Appendix*).

Parish Registers. After 1538 (ref. 29, p. 54, and ref. 30), London parish registers provide information on mortality. We use weekly counts of deaths published online by Cummins, which are estimated to cover 80% of total deaths (31). During plague epidemics, most deaths were likely due to plague; we also adjust for nonplague mortality by estimating a baseline death rate from the years before and after an epidemic (*Materials and Methods*).

Significance

Epidemics of plague devastated Europe's population throughout the Medieval and Renaissance periods. Genetic studies of modest numbers of skeletal remains indicate that the causative agent of all these epidemics was the bacterium *Yersinia pestis*, but such analyses cannot identify overall patterns of transmission dynamics. Analysis of thousands of archival records from London, United Kingdom, reveals that plague epidemics spread much faster in the 17th century than in the 14th century.

Author contributions: D.J.D.E., J.M., H.P., J.D., and B.M.B. designed research; D.J.D.E., J.M., J.D., and B.M.B. performed research; D.J.D.E., J.M., J.D., and B.M.B. contributed new analytic tools; D.J.D.E., J.M., J.D., and B.M.B. analyzed data; and D.J.D.E., H.P., J.D., and B.M.B. wrote the paper.

The authors declare no competing interest.

This article is a PNAS Direct Submission.

[1]To whom correspondence may be addressed. Email: earn@math.mcmaster.ca.

This article contains supporting information online at https://www.pnas.org/lookup/suppl/doi:10.1073/pnas.2004904117/-/DCSupplemental.

*The core genome is about 80% of the full genome, shared between all sequenced strains of *Y. pestis*.

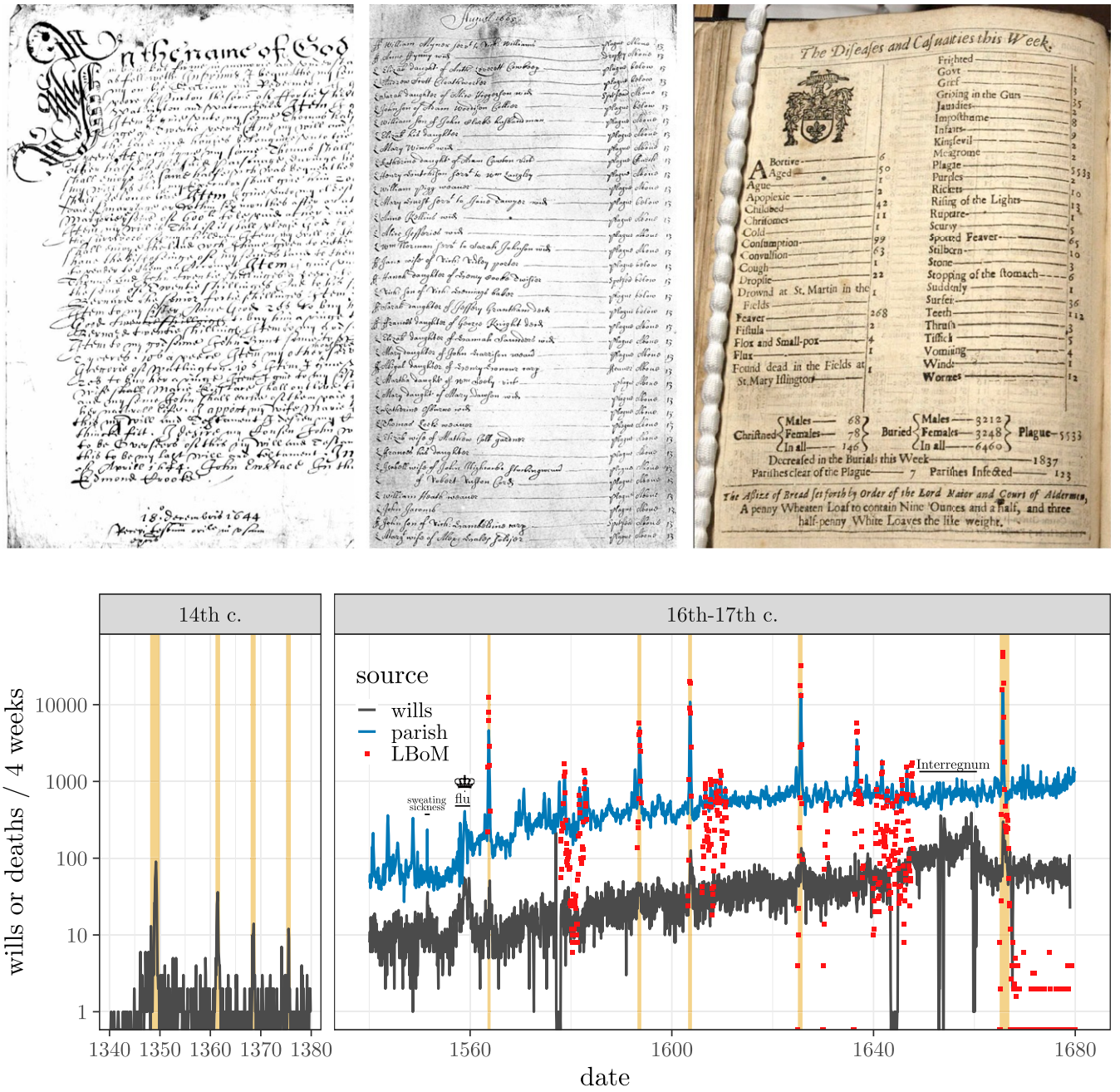

Fig. 1. (*Top Left*) Part of a will proved in the PCC, dated 18 December 1644 (34). (*Top Center*) A parish register page from St Giles without Cripplegate, August 1665 (38). Image credit: Wellcome Collection, licensed under CC BY 4.0. (*Top Right*) One of the LBoM, for the week beginning 26 September 1665 (photo by Claire Lees, taken in the Guildhall Library, City of London). (*Bottom*) Mortality in London, United Kingdom, 1340 to 1380 and 1540 to 1680, aggregated 4-weekly, plotted on a log scale. The three distinct sources of data (*SI Appendix*, Table S2) are last wills and testaments of Londoners whose wills were probated in the Court of Husting (14th century) or the PCC (16th to 17th centuries), weekly aggregations of burials listed in extant parish registers (29), and weekly plague deaths listed in the LBoM (27). Major plague years are highlighted in yellow. Aside from these and various minor plague years, there are notably unusual patterns during an epidemic of sweating sickness in 1551 (ref. 29, p. 70), the influenza epidemic of 1557 to 1559 (ref. 29, p. 70) (which coincided with the end of the reign of Bloody Mary I and the ascension of Elizabeth I in 1558 [indicated by a crown icon]), and the absence of a monarch during the Interregnum from 30 January 1649 to 29 May 1660.

Wills and Testaments. Before 1538, no direct tabulations of mortality for London are available. However, we do have detailed information on last wills and testaments, which can be used as proxies for mortality (29). In particular, we have digitized and tabulated daily counts of wills recorded in the Court of Husting (32) for the 14th century; these give us data for the plague epidemics of 1348, 1361, 1368, and 1375 [monthly counts for three of these epidemics were previously published by Cohn (33)]. We use online data from the Prerogative Court of Canterbury (PCC) (34) for the plague epidemics of the 16th and 17th century. Plague epidemics in London are mentioned in historical documents from the 15th century (ref. 27, chap. IV), but during this period, wills recorded in the Courts of Husting and Canterbury were too sparse to enable identification of epidemics.

Two dates are associated with each will: the date on which it was written and the date on which it was probated (i.e.,

accepted by the court after the death of the testator). Traditionally, demographers have used annual counts of wills by probate date as testators are known to have died by these dates. While this approach works well for inferring long-term trends in annual mortality, probate dates are inappropriate for reconstructing detailed time series of mortality over short time scales as there is a variable and irregular lag between the (unknown) date of the death and the probate date; most of the wills associated with 14th century epidemics were probated several months after they were written (35) (*SI Appendix*, Fig. S2).

Instead, we use the counts of wills written in a given time interval as a proxy for plague incidence. The date on which a will was written may precede the testator's death by a long period, but during severe epidemics, will dates were likely to have been correlated with the fear of infection (and hence with disease incidence), just as internet searches for influenza symptoms can predict 21st century epidemic patterns (36).

When using wills as proxies for mortality or incidence, we must keep in mind that 1) a much smaller proportion of the population is sampled (the will counts in Fig. 1 are about 10 times smaller than the counts based on parish registers) and 2) the subpopulation of individuals who wrote wills is strongly biased toward merchants and others who owned property (primarily males).

For the period since 1540, the existence of multiple sources allows us to cross-check results—in particular, to test our assertion that aggregated counts of wills by date written are an adequate proxy for mortality rates—and avoid relying on any questionable or poorly sampled segments of data (37) (*SI Appendix*). In 1563 and 1593, the number of PCC wills is too small to extract a signal from the noise, but the data for the later three outbreaks verify that the numbers of wills written follow the plague epidemic patterns evident in the mortality records (Fig. 2). Based on cross-correlation analysis and differences between epidemic peak times, will counts appear to have lagged mortality recorded in parish registers and LBoM by approximately 3 to 5 wk; our inferences about epidemic growth rates appear to be robust to this lag (*SI Appendix*).

The LBoM indicate that there were 18 other plague epidemics in London between 1563 and 1666; these were all of much smaller magnitude and are discussed only in *SI Appendix*. No plague epidemics have occurred in London since the end of the Great Plague in 1666: a total of 77 deaths from plague are recorded in the LBoM after 1666, never more than 5 in a single week. The last plague deaths recorded in the LBoM occurred during the week of 6 May 1679.

Approach

Estimation of Epidemic Growth Rates. While our collection of high-resolution mortality time series during plague epidemics allows us to estimate epidemic growth rates, we are constrained by the limitations of our data—the time series for each epidemic are short and noisy, especially during the 14th century (e.g., the epidemics of 1368 and 1375 peaked at a total of five wills written per week). Thus, we chose to use simple phenomenological models with a small number of parameters that can be fitted to short time series (starting size, growth rate, and total size; *Materials and Methods*) and do not attempt to separate different sources of variability or estimate the influence of various mechanistic processes [King et al.'s exhortation to use epidemic models that separate process from observation noise (39) applies primarily to forecasting, which we are not attempting]. Furthermore, we primarily consider the initial growth rate r, which—unlike the basic reproduction number $\mathcal{R}_0$—can be estimated reliably from mortality data alone without any knowledge of the disease characteristics or natural history (26).

We estimate the epidemic growth rate for each epidemic as the maximum likelihood estimate of the initial growth rate of a logistic function fitted to the cumulative death curve (using first differences to avoid overconfidence; see *Materials and Methods* for more detail), along with likelihood profile CIs. To summarize the overall difference between epochs, we then use the estimates

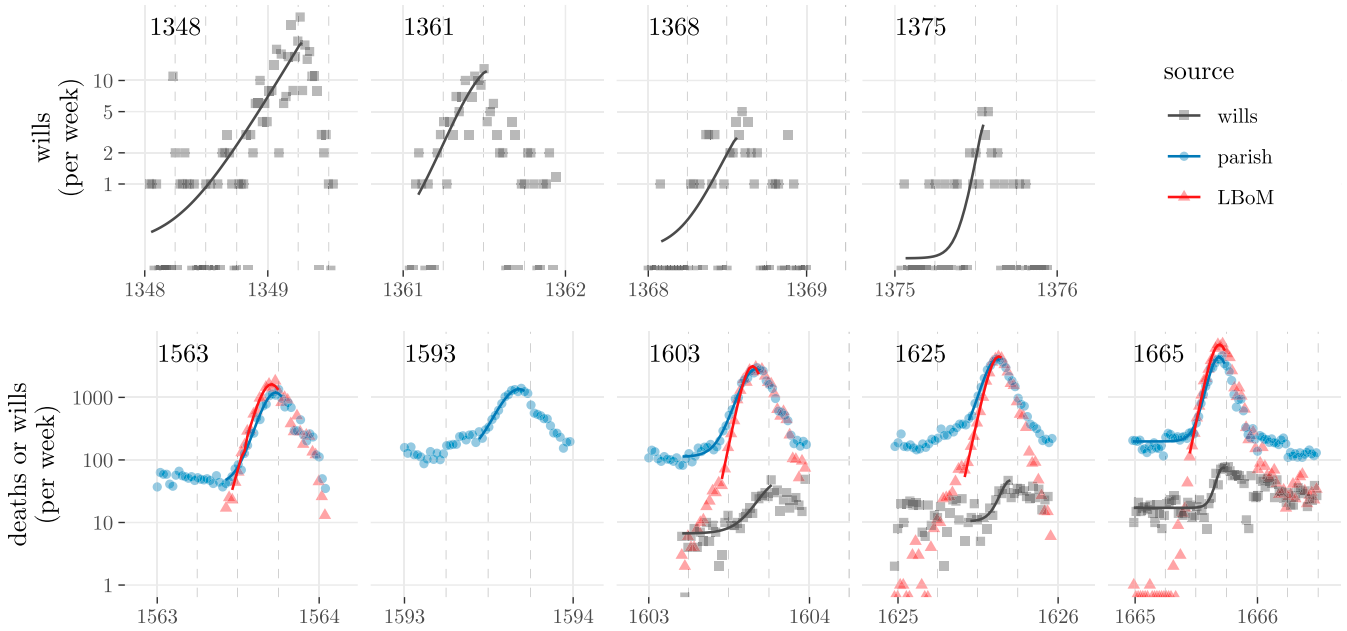

Fig. 2. Observed time series (points) and phenomenological model fits (lines; *Materials and Methods*) that yield the estimated growth rates (listed in Table 1 and plotted in Fig. 3). The data sources (*SI Appendix*, Table S2) are described in the main text and the legend of Fig. 1. For visual comparison, wills were aggregated weekly to match the frequency of mortality observations (fits to wills were based on the original daily counts). Vertical dashed lines show 1 April, 1 July, and 1 October of each year. Weeks with zero counts are shown along the bottom edge of the graph (present in all 14th century epidemics, 1625, and 1665). *SI Appendix*, Figs. S5 and S6, display the data during the major plague epidemics on linear rather than logarithmic scales.

for each epidemic as observations in a linear mixed model including fixed effects of epoch (early/14th century vs. late/16th to 17th centuries) and data source, and a random effect of outbreak year (see below), where each estimate was weighted by its certainty.

Finally, to robustly quantify the statistical significance of the difference between epochs, we ran a permutation test. We computed the null distribution of the between-epoch difference in growth rate by scrambling the estimates and associated CIs randomly across epochs. For each of the 126 possible permutations, we refitted the mixed model and extracted the estimated among-epoch difference in growth rate.

Estimating $\mathcal{R}_0$ and Attack Rate. Our analysis focuses on the epidemic growth rate r, rather than the more commonly investigated basic reproduction number $\mathcal{R}_0$ [the expected number of secondary cases caused by a primary case in a completely susceptible population (7)], because estimates of $\mathcal{R}_0$ depend on information about the life history of the pathogen as well as on the epidemic curve itself (40). However, if we can estimate $\mathcal{R}_0$, then we can predict epidemic outcomes that we are unable to predict from r alone; then, by comparing observed with theoretical outcomes under different scenarios, we can make inferences about modes of transmission.

In particular, if the host population is homogeneously mixed, we can use $\mathcal{R}_0$ to estimate the expected final size Z (the proportion of the population infected by the end of an epidemic, also called the attack rate) (6, 41). The observed attack rate based on mortality records depends in turn on the fraction of infected individuals who die from disease. We can thus compare theoretical expectations of observed attack rates under different transmission modes with historical information about observed attack rates (see *Implications of Growth Rate Estimates for Transmission Mode*).

We can use the distribution of the generation interval (the times elapsed between the moment a host is infected and the times at which they infect others) to compute $\mathcal{R}_0$ from r (40). If we know only the mean generation interval T_g, we can still approximate $\mathcal{R}_0 \approx rT_g + 1$, by assuming that the generation intervals are exponentially distributed; this approximation underestimates $\mathcal{R}_0$ in the typical case where the generation interval distribution is less variable than an exponential distribution with the same mean.

Beyond the information on generation interval that we use to derive $\mathcal{R}_0$ from r, the observed attack rate depends on additional characteristics of an epidemic. If the population does not mix homogeneously, the final size will typically decrease (e.g., figure 6 in ref. 42). Since the case fatality proportion (CFP; the proportion of plague cases who die) is not 100%, the observed attack rate is less than the final size. Observed attack rates also decrease if some individuals are infected without showing symptoms (asymptomatic infections) (43) or without symptoms identified as plague (subclinical infections). Finally, the observed attack rate depends on the initial proportion of the population susceptible, which will be lower if some individuals have previously acquired immunity after prior nonfatal plague infections.

We can use independent estimates of the generation interval to estimate $\mathcal{R}_0$ (and hence the theoretical attack rate) for London epidemics under different transmission modes. Given the limited information that we have, we consider the additional (extreme) assumptions that 1) the population was homogeneously mixed, 2) the population was initially 100% susceptible, 3) there were no asymptomatic infections, and 4) all infected individuals died (i.e., the CFP was 100%). All of these assumptions increase the observed attack rate (as detected from wills or deaths), so we can calculate an upper bound on the total mortality we would expect to observe in an epidemic with a particular transmission mode.

Results

The fitted models do as good a job as one could hope for in capturing the initial patterns of epidemic growth evident in the noisy will counts and agree very well with the patterns of growth in the mortality time series that are available in the later epoch (Fig. 2).

The growth rates for the 14th century epidemics are lower than those for the 16th to 17th centuries (Fig. 3); they may also be more variable than in the later period, although some of the appearance of variability is due to larger uncertainties (presumably due to the relatively poor sampling in the early epoch). The mixed model quantifies the dramatic increase in growth rate ("acceleration") of epidemics between epochs. The growth rates increased fourfold in the late vs. early epochs: r increased $3.9\times$ [95% CI $(1.5\times, 10.3\times)$] (*Materials and Methods*). The permutation test results support the statistical significance of this difference; the observed order of outbreaks yields the most extreme difference in growth rates out of all 126 possible orderings, giving a two-tailed P value of $2/126 = 0.016$.

Discussion

Plague epidemics in London appear to have been faster in the 16th to 17th centuries than in the 14th. Our analysis shows that this difference is very likely real, rather than driven by changes in the types of documentary evidence that are available; in particular, we have shown that inferences from will counts are consistent with those from death counts when both are available, in the 17th century.

Why the later plague epidemics were faster than the earlier ones is not clear. Nevertheless, to provide some context, we consider below a number of mechanisms that could have contributed to increases in epidemic growth rates. We then consider what our estimated epidemic growth rates suggest about the mode of transmission during the various London plague epidemics.

Possible Causes of Acceleration. What factors could have caused plague epidemics in London in the 16th and 17th centuries to accelerate relative to the earlier plagues in the 14th century?

Pathogen or host evolution. Faster growth could be a consequence of the pathogen evolving to infect hosts more effectively or to remain infectious for longer. However, such evolution may be challenging to demonstrate, particularly in light of the strong genetic similarity between the Second Pandemic and Modern Plague strains (21). Evolution of host resistance has also been suggested as a cause of changes in plague dynamics (11), although we have no particular mechanisms in mind for how the evolution of resistance over the course of centuries could accelerate epidemics.

Shifts in transmission mode. Modes of transmission may have differed between epochs, which could account for differences in epidemic growth rates. The reservoir host of *Y. pestis* in London was rat populations where it was primarily spread by flea vectors such as *Xenopsylla cheopis* (ref. 14, p. 54). This transmission mode gives rise to bubonic plague in humans, as a consequence of zoonotic spillover; epidemic growth rate is driven by spread among rats and fleas, with human infection and mortality as a secondary consequence. In contrast, when *Y. pestis* infection in humans spreads to the lungs, it gives rise to pneumonic plague, which can then spread directly from human to human like other severe respiratory infections. It has also been more recently hypothesized that human ectoparasites (including lice and human fleas) could have supported indirect plague transmission without involving rats (13, 45).

Pneumonic plague probably has shorter generation intervals than bubonic plague (44, 46) and is often thought to spread much faster at the population level (44); one potential explanation for our observations is that 14th century epidemics were primarily

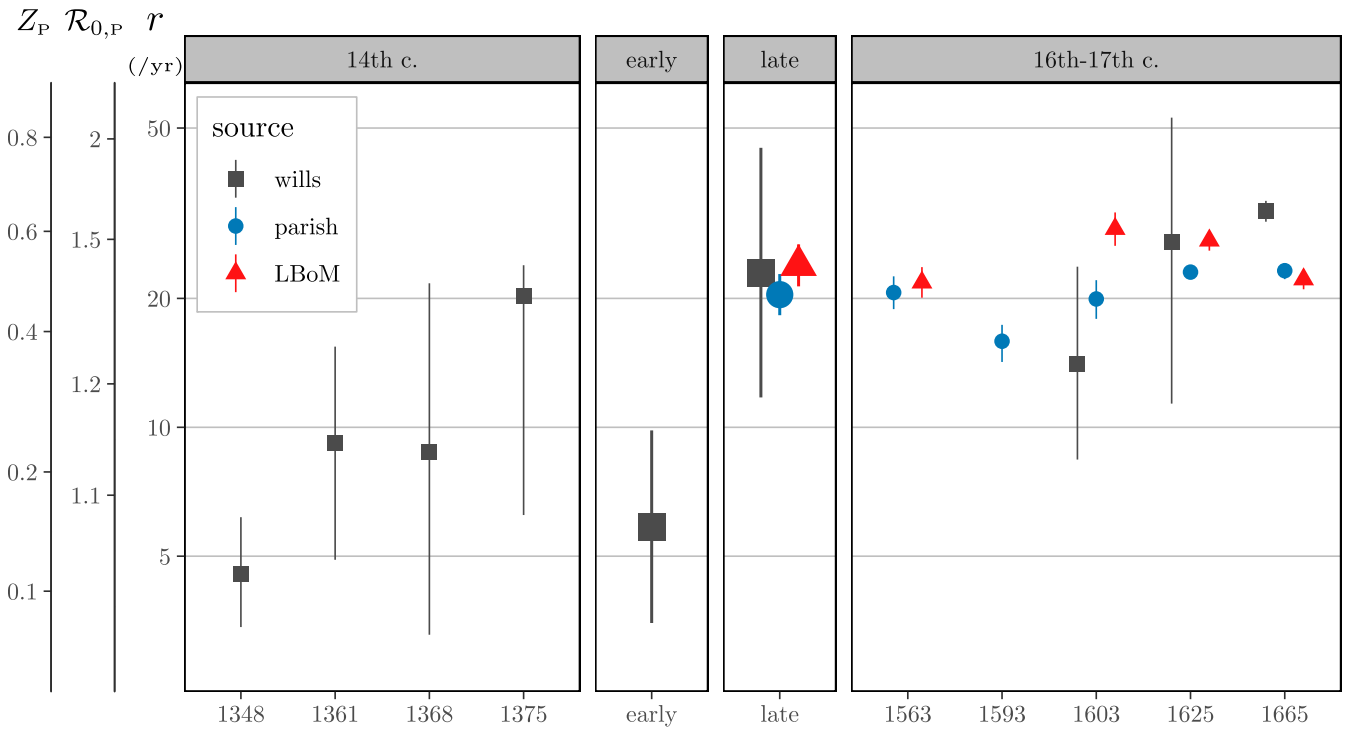

Fig. 3. Estimated initial growth rates (r) and 95% profile CIs on a logarithmic scale, for each of the epidemics shown in Fig. 2. Second and third panels show mixed-model estimates (*Materials and Methods*) of overall average growth rate for each epoch (early, 14th century vs. late, 16th to 17th centuries) and data source. To aid interpretation, the additional vertical scales show the implied intrinsic reproductive number ($\mathcal{R}_{0,P}$) and epidemic final size (Z_P) under the assumption that the generation interval distribution (40) was the same as that estimated from 20th century pneumonic plague epidemics (44). All estimates and CIs are listed in Table 1 (which also lists the associated doubling times).

bubonically transmitted, while 16th to 17th century epidemics were primarily pneumonic. With currently available data, we are unable to confirm or reject this hypothesis, but we consider below whether any inferences about transmission mode can be made at present.

Ecological and demographic changes. The complete multispecies ecology of *Y. pestis* is extremely complicated (47). We focus on humans and not on the rest of the ecological community supporting *Y. pestis* because the only data available for the epochs studied here concern humans. Human population size and population density in London increased enormously from the 14th to 17th centuries (48–50) (*SI Appendix*, Table S1 and Fig. S1), and density increases were exacerbated in the 17th century by the isolation of the sick and their contacts in pest houses (51). Since bubonic plague epidemics are driven by spillover from rat–flea epidemics, human population density would only have a direct effect on the speed of pneumonic epidemics. However, changes in human population (and living conditions) almost certainly affect rat, and flea, density (52). In addition, higher rat densities make it more likely that fleas departing dying rats end up on susceptible rat hosts. The magnitudes of these effects are extremely difficult to estimate, but in *SI Appendix* we explore them in a (crude) quantitative manner, without attempting to model the truly complex population dynamics that occur even during a single epidemic (46, 53).

Environmental change. The external environment represents the third side of the host–parasite–environment disease triangle (54). Northern European climates changed significantly between the 14th and 16th to 17th centuries (the coldest period of the Little Ice Age occurred in the 17th century; ref. 55 and figure 1 of ref. 56). Furthermore, late-epoch epidemics occurred later in the calendar year and hence in different seasons (Fig. 2). A variety of studies link climate (e.g., overall wetness/dryness) or weather (e.g., annual precipitation or temperature) to plague incidence or transmission (57–63). Climatic changes may have been responsible for the changes in plague epidemics in London between 1348 and 1666, but it is challenging to make reliable inferences due to the lack of consensus about climate and weather variations in Medieval/Renaissance Europe (64).

Implications of Growth Rate Estimates for Transmission Mode. One might hope to exploit ancient DNA (2, 21) to identify the transmission mode during London plague epidemics. Unfortunately, there are currently no identified genetic differences between strains that have caused indirect or direct transmission, so it will be difficult to determine from genetic analyses whether one mode or the other was dominant in any given Medieval/Renaissance epidemic.

Our growth rate estimates provide a starting point from which we can begin to explore the extents to which direct or indirect transmission played a role in the various London plague epidemics. Current data are too sparse and limited to make precise predictions (26, 65), but we consider the extremes of estimated parameter ranges that would favor each mode of transmission and ask whether the resulting predictions of attack rates are consistent with the rough knowledge of epidemic sizes available from the literature.

In the early epoch, primarily pneumonic transmission is implausible. If we assume pneumonic transmission and use generation interval estimates from 20th century outbreaks (44) (i.e., assuming that the natural history of infection in London was similar to that of Modern pneumonic plague), in the early epoch we find $\mathcal{R}_{0,P} = 1.1$ [CI (1.04, 1.16)], which implies an attack rate of $Z_P = 15\%$ [CI (7.5%, 27%)] (left axes in Fig. 3). This estimate of total mortality is the largest possible for the early-epoch epidemics (violations of any of the four extreme assumptions

Table 1. Maximum likelihood estimates (MLEs) of the initial exponential growth rate (r) and doubling time ((log 2)/r) with their 95% CIs, obtained from the time series shown in Fig. 2 (see *Materials and Methods*)

				Assuming pneumonic plague		
Source	Epidemic	Growth rate (1/y)	Doubling time (days)	$\mathcal{R}_{0,P}$	Attack rate Z_P	R^2
Husting wills	1348	4.5 (3.4, 6.2)	55.6 (41.1, 74.1)	1.06 (1.04, 1.09)	0.11 (0.08, 0.16)	0.439
Husting wills	1361	9.2 (4.9, 15.4)	27.5 (16.4, 51.6)	1.14 (1.07, 1.25)	0.23 (0.12, 0.37)	0.693
Husting wills	1368	8.4 (3.3, 21.7)	30.2 (11.7, 77.2)	1.12 (1.04, 1.38)	0.21 (0.08, 0.49)	0.333
Husting wills	1375	20.3 (6.0, 60.3)	12.5 (4.2, 42.2)	1.35 (1.08, 2.41)	0.47 (0.15, 0.88)	0.669
London bills	1563	21.8 (20.1, 23.7)	11.6 (10.7, 12.6)	1.38 (1.34, 1.42)	0.49 (0.46, 0.52)	0.961
London parish	1563	20.6 (18.9, 22.5)	12.3 (11.2, 13.4)	1.35 (1.32, 1.39)	0.47 (0.44, 0.51)	0.978
London parish	1593	15.9 (14.2, 17.3)	15.9 (14.6, 17.8)	1.26 (1.23, 1.29)	0.38 (0.35, 0.41)	0.986
Canterbury wills	1603	14.0 (8.3, 23.8)	18.0 (10.6, 30.4)	1.23 (1.12, 1.42)	0.34 (0.21, 0.53)	0.853
London bills	1603	29.1 (26.5, 31.8)	8.7 (8.0, 9.5)	1.54 (1.48, 1.60)	0.61 (0.57, 0.64)	0.927
London parish	1603	19.9 (18.2, 21.8)	12.7 (11.6, 13.9)	1.34 (1.30, 1.38)	0.46 (0.43, 0.49)	0.988
Canterbury wills	1625	27.1 (11.4, 53.5)	9.3 (4.7, 22.3)	1.49 (1.18, 2.19)	0.58 (0.28, 0.84)	0.900
London bills	1625	27.3 (25.9, 28.4)	9.3 (8.9, 9.8)	1.50 (1.46, 1.52)	0.58 (0.56, 0.60)	0.996
London parish	1625	23.0 (22.3, 23.7)	11.0 (10.7, 11.3)	1.40 (1.39, 1.42)	0.51 (0.50, 0.53)	0.999
Canterbury wills	1665	35.8 (17.6, 47.5)	7.1 (5.3, 14.4)	1.69 (1.29, 2.01)	0.69 (0.42, 0.80)	0.842
London bills	1665	22.2 (21.0, 23.4)	11.4 (10.8, 12.0)	1.39 (1.36, 1.41)	0.50 (0.48, 0.52)	0.984
London parish	1665	23.2 (20.6, 26.0)	10.9 (9.7, 12.3)	1.41 (1.35, 1.47)	0.52 (0.47, 0.56)	0.987
Husting wills	Early	5.9 (3.5, 9.8)	43.2 (25.7, 72.5)	1.08 (1.04, 1.15)	0.15 (0.08, 0.25)	
Canterbury wills	Late	23.0 (11.7, 45.0)	11.0 (5.6, 21.5)	1.40 (1.18, 1.94)	0.51 (0.29, 0.78)	
London bills	Late	23.9 (21.3, 26.7)	10.6 (9.5, 11.9)	1.42 (1.37, 1.48)	0.53 (0.49, 0.57)	
London parish	Late	20.4 (18.3, 22.8)	12.4 (11.1, 13.8)	1.35 (1.31, 1.40)	0.47 (0.43, 0.51)	

The goodness of fit measure (R^2) is the proportional reduction in the mean squared error, i.e., $1 - d^2/\sigma^2$ where d^2 is the model mean squared error and σ^2 is the (population) variance of the data; predictions and observations are aggregated to weekly before computing the R^2 for wills, for consistency among data sources. The implied basic reproduction numbers ($\mathcal{R}_{0,P}$) and attack rates (Z_P), assuming the generation interval distribution for Modern pneumonic plague (44), are also shown. All MLEs and associated CIs are shown in Fig. 3.

discussed in *Approach* would lower the total mortality). Total mortality of 15% is implausibly low in comparison to typical estimates for 14th century plague epidemics [e.g., "[b]etween the years 1346 and 1352, [plague] caused the death of ... one-third of the world's population at that time" (ref. 19, p. 163)] and certainly inconsistent with the careful and comprehensive analysis of Creighton for the 1348 to 1349 epidemic in London specifically ["the mortality was about one-half the population" (ref. 27, p. 128)]. It is therefore unlikely that 14th century plague epidemics in London were primarily pneumonic.

In the early epoch, growth rates appear to be consistent with bubonic plague. What if we assume bubonic transmission? Unfortunately, the expected total human mortality from a bubonic plague epidemic depends on several poorly known aspects of rat ecology. For the generation interval T_g for bubonic plague we use a rough estimate of 18 d (≈ 0.05 y) based on the flea incubation period of 9 to 26 d (46), which dominates the time scales of other processes involved in rat–flea plague dynamics (see *SI Appendix* for further detail). In combination with a growth rate estimate of $r \approx 6$/y, we obtain $\mathcal{R}_{0,B} \approx 1.3$ and $Z_B \approx 42\%$. However, this estimate of the final size gives the fraction of rats, not humans, infected over the course of the epidemic. Translating this rat final size to the final size of the human epidemic requires us to quantify the amount of spillover from rats to humans. In particular, we need to know the rat-to-human ratio and the number of infected humans per infected rat, which can both be crudely estimated as 1:1 (53) (although these ratios will vary during the course of plague epidemics). Given an estimated CFP of 70 to 80% for early-epoch plagues (66), our (very rough) mortality predictions are reasonably consistent with the observed human mortality rates.

In the late epoch, primarily pneumonic transmission is unlikely but cannot be ruled out. Now suppose that the late-epoch plagues were pneumonic with a generation interval similar to that of Modern pneumonic plague. The implied reproduction number (Fig. 3) would be $\mathcal{R}_{0,P} = 1.4$ [CI (1.2, 2.1)], which yields a maximum attack rate of 51% [CI (27%, 81%)], compared to the estimated $\approx 20\%$ of the population who died in each of the late-epoch epidemics (ref. 31, p. 4). Given that the CFP for (Modern) pneumonic plague is nearly 100% (20, 67–69), reconciling the predicted attack rates with observed mortality would require strong effects of heterogeneity, a large fraction of individuals resistant to plague due to prior nonfatal plague infections, a large proportion of asymptomatic or subclinical infections, or a decrease in transmission rate as the plague spread (perhaps due to behavioral avoidance of transmission). The effects of heterogeneity and behavioral avoidance may indeed have been stronger in the late epoch, as a result of concentration of the wealthy in central London and a tendency for them to flee London during plague epidemics (ref. 31, p. 4). While we still consider direct (pneumonic) transmission in late-epoch London plague epidemics unlikely because of the strong effects that would be needed to reduce the expected mortality rates to the observed levels, we cannot rule it out.

In the late epoch (as in the early epoch), growth rates appear to be consistent with bubonic plague. Similar calculations with the estimated r for the late epoch and the approximate generation interval for bubonic plague give estimated $\mathcal{R}_{0,B} = 2.1$ [CI $(1.5, 3.5)$] and predicted rat attack rates of $Z_B = 83\%$ [CI $(61\%, 96\%)$]. The human Z_B would be identical, if we were to make the same assumptions as above. This attack rate is even higher than the 51% predicted for pneumonic plague, but the CFP for bubonic plague was probably only 30 to 60% in the 16th to 17th centuries (e.g., refs. 19 and 69), which could bring the total mortality roughly in line with the observed $\approx 20\%$. The lower CFP of bubonic plague would also lead to a build-up in the population of individuals who had survived previous plague epidemics and retained immunity (reducing the susceptible population available to be attacked), which in combination with heterogeneity and asymptomatic infections makes bubonic transmission plausible for the late epoch.

Other possibilities. As mentioned above, it is possible that human ectoparasites could have supported indirect plague transmission (13, 45). While the biological details of this transmission mode are still uncertain, we can guess that the generation interval of this transmission mode would be intermediate between direct and indirect rat–flea transmission, giving rise to estimates of $\mathcal{R}_0$ and Z intermediate between those discussed above. Investigations of plague biology in fleas have also raised the possibility that rat transmission may have shorter generation intervals than previously thought, which would lower estimated $\mathcal{R}_0$ values for bubonic plague (70, 71) (but cf. ref. 72).

COVID-19 Context. The world is currently in the midst of a pandemic of COVID-19 disease, caused by the SARS-CoV-2 virus (73). The infection fatality ratio (IFR) for COVID-19 is uncertain due to case detection limitations, but the evidence accumulated to date about this IFR (74, 75) indicates that it is substantially lower than for the 1918 influenza (76, 77) and much lower than for the historical plague epidemics studied here. Nevertheless, COVID-19 has had a much greater impact than seasonal influenza epidemics, which cause of order 500,000 deaths worldwide annually (76, 78).

Epidemic growth rates (and doubling times) have been important elements of the COVID-19 public health discourse (79). The quality and quantity of COVID-19 data far exceed that of the historical plague data we have analyzed in this paper. In particular, many countries report daily counts of newly reported cases, hospitalizations, and deaths. The techniques we have used to estimate initial growth of plague outbreaks are consequently easier to apply to modern data streams and should yield more accurate estimates. In addition, improved information about generation intervals will make it easier to convert growth rate estimates into estimates of the basic reproduction number $\mathcal{R}_0$. Of course, modern data are by no means perfect, and there are still many issues—including estimating generation intervals while accounting for disease dynamics, and assessing the importance of asymptomatic and presymptomatic transmission—that can lead to overconfident or incorrect estimates of disease parameters for COVID-19 (79–81).

Conclusion. We have estimated epidemic growth rates for all of the recorded plague epidemics in London, United Kingdom, during the second pandemic (1348 to 1666). The major plagues of the 16th and 17th centuries grew much faster than the early plagues of the 14th century when the Black Death first invaded human populations. This conclusion is based solely on estimated growth rates—in particular, our estimates do not rely on assumptions about the mode of transmission or natural history of infection. The cause of this substantial acceleration is currently unclear.

We considered the implications of our estimated growth rates with respect to the mode of transmission and concluded that direct transmission (pneumonic plague) was unlikely to have been the primary mode in the early epoch. Definite conclusions about indirect transmission (bubonic plague) are difficult because of the substantial uncertainties about rat and flea ecology during this period.

We have created and assembled—and made available with this paper—machine-readable databases composed of thousands of handwritten records spanning more than 300 y. People living in London in 1348 or 1665 could not have imagined how these records might be used hundreds of years later. The time series that have emerged have allowed us to reveal and characterize large changes in patterns of infectious disease transmission. In concert with other forms of information (31, 82), these records should continue to contribute to a broader and more insightful view of population-level processes in early eras of history.

Materials and Methods

Growth Rate Estimates. We have previously developed methods to use mortality data to estimate initial epidemic growth rates (26). The naïve approach of fitting a straight line to the relationship between logarithmic death counts and time at the beginning of the epidemic depends sensitively on the fitting window and produces overly narrow confidence intervals. Instead, we use maximum likelihood estimation to fit a curve that resembles the shape of a deterministic epidemic model (see *Phenomenological Model*) and compute likelihood profile confidence intervals (83); this approach yields robust estimates of initial growth rates and accurate assessments of uncertainty. All variation around the fitted line is assumed to arise from observation errors. See Ma et al. (26) for methodological details.

In contrast to Ma et al. (26), who assumed a Poisson error model to fit simulations that were themselves generated with that assumption, the results shown here applied a negative binomial error model, which allows for the broader range of variation found in real data. We initially tried both logistic and Richards (84) models for the epidemic curve (i.e., the expected mean of the data) and both Poisson and negative binomial models for the distribution around the mean. These variants gave qualitatively similar conclusions about the pattern of growth rates, but we found that the Richards model was too unstable to fit reliably across all epidemics, so we reverted to fitting the logistic model for all epidemics. Similarly, the negative binomial model gave unstable results when the distributions were too close to Poisson; when the negative binomial dispersion parameter was estimated as $> 10^4$, we reverted to a Poisson fit (see *SI Appendix* for further details of the optimization).

In order to summarize the differences between epochs, we fitted a linear mixed model [using the glmmTMB package in R (85)] to the estimates of log growth rates. To account for differing precision of the estimates across epidemics, we approximate the SE of the estimates as the width of the 95% confidence interval divided by 3.92 (the width in standard errors of a 95% normal CI), square it to find the variance, and scale the residual variance for each epidemic curve by this observed variance. This procedure is equivalent to weighting each epidemic curve by the inverse of its variance. We quantified the difference in epidemic growth rate between epochs based on the predicted difference in $\log(r)$ between wills in each epoch.

The permutation test P value (0.016) reinforces our confidence that late-epoch epidemics were faster than early-epoch epidemics; however, since it is larger than the parametric P values derived from the model fit (which are < 0.001), it suggests that the confidence intervals shown in Fig. 3 may be too narrow.

In light of recent work investigating the possibility of initial epidemic growth that is subexponential, we also considered fits based on the more general growth model of Chowell and coworkers (86–88). This approach leads to slightly slower initial growth estimates but does not change our conclusion that the later plagues were much faster than the earlier plagues.

Phenomenological Model. Following Ma et al. (26), we model the cumulative mortality curve (or will-accumulation curve; henceforth, we refer to wills or death records as "mortality") using a logistic model with an added baseline linear growth rate,

$$c(t) = bt + \frac{K}{1 + [(K/c_0) - 1]e^{-rt}}. \quad [1]$$

Here $c_0 = c(0)$ is the initial cumulative mortality, r is the initial exponential growth rate, and K is the final size of the epidemic ($\lim_{t\to\infty}[c(t) - bt]$). In the fitting procedure we use the unitless parameter $x_0 = c_0/K$; all parameters are fitted on a transformed, unconstrained scale [i.e., $\log(r)$, $\log(K)$, and $\operatorname{arctanh}(x_0)$]. The derivative $c'(t)$ is the instantaneous mortality rate. To avoid the inherent correlations between observations in the cumulative curve, we fit the observed data to the differences from Eq. **1**: $\Delta c(t) = c(t + \Delta t) - c(t)$, where Δt is the observation interval (1 d for wills and 1 wk for mortality data). The parameter b represents baseline (nonplague) mortality. For the LBoM fits we set $b = 0$ (since the LBoM data include only plague mortality); for the wills and parish register fits we estimated b by computing the average observed mortality rate over the 2 y preceding and following the outbreak window (see *Outbreak Years and Outbreak Windows*).

As discussed above, we initially fitted a Richards model, which extends the logistic equation with a shape parameter, but found that we could not get stable fits to the smallest/noisiest epidemics; we never found qualitative differences between growth rates estimated from logistic and Richards fits.

Ma et al. (26) found that a delayed logistic curve, which adds an exponentially distributed delay between infection and mortality, estimated growth rates from mortality curves with less bias. However, the delay between infection and mortality in our data is extremely uncertain—it would represent another parameter that would have to be estimated from noisy data. For wills data, the delay could even be negative; i.e., wills could have been written out of fear of future infection. Furthermore, because we found little difference between the Richards and logistic fits—which Ma et al. (26) found to have opposite biases—growth rates estimated by these two methods are likely to bracket the growth rate estimated by the delayed logistic.

Fitting Windows. How well a given model can fit a time series may depend on the time window used for fitting (88). In order to avoid choosing a window separately for each individual epidemic, we considered window selection criteria that could be applied uniformly to all epidemics without first examining the data. In all cases we defined the end of the fitting window to be one data point past the observed peak date (the date of maximum observed deaths). For wills and parish registers, we began the fitting window at the start of the outbreak window (see below); for LBoM data, we started immediately after the last observation before the peak for which the mortality rate was $\leq 1/50$ of the peak mortality rate. For two epidemics for which the data are particularly noisy (1593 and 1625), we were unable to find any simple heuristic that would automatically choose a good fitting window and resorted to choosing the fitting window by eye.

The fitting windows used for all our fits are listed in *SI Appendix*, Tables S6 and S7. Although we experimented with different methods for determining the fitting window (e.g., starting the window from the observation after the last local minimum before the peak or based on a threshold of $1/100$ of the peak mortality rate), we emphasize that our choices were entirely determined by seeking good fits (judged by visual inspection) and not by the pattern of estimated initial growth rates. Moreover, our conclusion that later plagues were much faster than the earlier plagues is robust to choices we made about window selection.

Outbreak Years and Outbreak Windows. We refer to the calendar year in which an epidemic begins as the outbreak year. For each epidemic, we define an outbreak window that is the maximum time interval to be considered for fitting. For the 14th century epidemics, we defined the outbreak window to be the full outbreak year, except for outbreak year 1348 when the epidemic spanned both 1348 and 1349 (so we took the outbreak window to be the full length of both calendar years). For the late-epoch epidemics, we defined the outbreak windows as sequences of consecutive weeks during which at least one plague death was listed in the LBoM (*SI Appendix*, Tables S6 and S7).

Data and Code Availability. Our epigrowthfit R package for estimating initial growth rates, which includes all of the data used in this paper, is available in Github at https://github.com/davidearn/epigrowthfit. The data can also be obtained from the International Infectious Disease Data Archive (http://iidda.mcmaster.ca). The additional code required to reproduce all of our results is available in Github at https://github.com/davidearn/plague_growth.

ACKNOWLEDGMENTS. The plague mortality data were photographed and/or entered by Seth Earn, Kelly Hancock, Claire Lees, James McDonald, David Price, and Hannah Price. Valerie Hart facilitated research and photography at the Guildhall Library, City of London. Nonexponential comparison fits were conducted by David Champredon. Sang Woo Park assisted in finding published estimates of auxiliary epidemic parameters. Alexandra Bushby assisted with compiling probate dates. Sigal Balshine, Ann Carmichael, and David Price made helpful comments. Early stages of this research were supported by a J. S. McDonnell Foundation Research Award to D.J.D.E. (https://www.jsmf.org/grants/d.php?id=2006014). All of the authors were supported by Discovery grants from the Natural Sciences and Engineering Research Council of Canada. H.P. was supported by the Social Sciences and Humanities Research Council of Canada. The Shared Hierarchical Academic Research Computing Network (SHARCnet; http://www.sharcnet.ca) provided computational resources. D.J.D.E. dedicates this paper to Josephine Earn, who enthusiastically discussed the history of London (and plagues) with him over many years.

1. W. H. McNeill, *Plagues and Peoples* (Anchor Books, New York, 1976).
2. D. M. Wagner *et al.*, *Yersinia pestis* and the Plague of Justinian 541-543 AD: A genomic analysis. *Lancet Infect. Dis.* **14**, 319–326 (2014).
3. S. Pepys, *The Diary of Samuel Pepys, 1660–1669*. https://www.pepysdiary.com/diary/. Accessed 22 September 2020.
4. R. Latham, *The Shorter Pepys* (University of California Press, Berkeley, 1985).
5. D. Defoe, *A Journal of the Plague Year*. http://www.gutenberg.org/ebooks/376. Accessed 22 September 2020.
6. W. O. Kermack, A. G. McKendrick, A contribution to the mathematical theory of epidemics. *Proc. R. Soc. Lond. A* **115**, 700–721 (1927).
7. R. M. Anderson, R. M. May, *Infectious Diseases of Humans: Dynamics and Control* (Oxford University Press, Oxford, 1991).
8. M. J. Keeling, C. A. Gilligan, Metapopulation dynamics of bubonic plague. *Nature* **407**, 903–906 (2000).
9. N. Bacaër, The model of Kermack and McKendrick for the plague epidemic in Bombay and the type reproduction number with seasonality. *J. Math. Biol.* **64**, 403–422 (2012).
10. O. Silva, Black Death—Model and simulation. *J. Comput. Sci.* **17**, 14–34 (2016).
11. J. A. Lewnard, J. P. Townsend, Climatic and evolutionary drivers of phase shifts in the plague epidemics of colonial India. *Proc. Natl. Acad. Sci. U.S.A.* **113**, 14601–14608 (2016).
12. R. P. H. Yue, H. F. Lee, C. Y. H. Wu, Navigable rivers facilitated the spread and recurrence of plague in pre-industrial Europe. *Sci. Rep.* **6**, 34867 (2016).
13. K. R. Dean *et al.*, Human ectoparasites and the spread of plague in Europe during the Second Pandemic. *Proc. Natl. Acad. Sci. U.S.A.* **115**, 1304–1309 (2018).
14. R. D. Perry, J. D. Fetherston, *Yersinia pestis*—Etiologic agent of plague. *Clin. Microbiol. Rev.* **10**, 35–66 (1997).
15. S. Neerinckx, E. Bertherat, H. Leirs, Human plague occurrences in Africa: An overview from 1877 to 2008. *Trans. R. Soc. Trop. Med. Hyg.* **104**, 97–103 (2010).
16. World Health Organization, Human plague: Review of regional morbidity and mortality, 2004-2009: Introduction. *Wkly. Epidemiol. Rec.* **85**, 40–45 (2010).
17. European Centre for Disease Prevention and Control, *Plague Outbreak, Madagascar, 2017* (European Centre for Disease Prevention and Control, Stockholm, 2017), pp. 1–10.
18. L. Roberts, Echoes of Ebola as plague hits Madagascar. *Science* **358**, 430–431 (2017).
19. B. L. Ligon, Plague: A review of its history and potential as a biological weapon. *Semin. Pediatr. Infect. Dis.* **17**, 161–170 (2006).
20. Centers for Disease Control and Prevention, Emergency preparedness and response: Frequently asked questions (FAQ) about plague. https://emergency.cdc.gov/agent/plague/faq.asp. Accessed 11 June 2018.
21. K. I. Bos *et al.*, A draft genome of *Yersinia pestis* from victims of the Black Death. *Nature* **478**, 506–510 (2011).
22. O. J. Benedictow, *What Disease was Plague? On the Controversy over the Microbiological Identity of Plague Epidemics of the Past* (Brill's Series in the History of the Environment, Brill, 2011), vol. 2.
23. T. Butler, Plague history: Yersin's discovery of the causative bacterium in 1894 enabled, in the subsequent century, scientific progress in understanding the disease and the development of treatments and vaccines. *Clin. Microbiol. Infect.* **20**, 202–209 (2014).
24. V. J. Schuenemann *et al.*, Targeted enrichment of ancient pathogens yielding the pPCP1 plasmid of *Yersinia pestis* from victims of the Black Death. *Proc. Natl. Acad. Sci. U.S.A.* **108**, E746–E752 (2011).
25. A. M. Devault *et al.*, Second-pandemic strain of *Vibrio cholerae* from the Philadelphia cholera outbreak of 1849. *N. Engl. J. Med.* **370**, 334–340 (2014).
26. J. Ma, J. Dushoff, B. M. Bolker, D. J. D. Earn, Estimating initial epidemic growth rates. *Bull. Math. Biol.* **76**, 245–260 (2014).
27. C. Creighton, *A History of Epidemics in Britain* (Frank Cass & Co. Ltd., London, ed. 2, 1965), vol. 1.
28. J. H. Tien, H. N. Poinar, D. N. Fisman, D. J. D. Earn, Herald waves of cholera in nineteenth century London. *J. R. Soc. Interface* **8**, 756–760 (2011).
29. P. Slack, *The Impact of Plague in Tudor and Stuart England* (Clarendon Press, Oxford, reprint, 1990).
30. R. Wall, English population statistics before 1800. *Hist. Fam.* **9**, 81–95 (2004).
31. N. Cummins, M. Kelly, C. Ó Gráda, Living standards and plague in London, 1560–1665. *Econ. Hist. Rev.* **69**, 3–34 (2016).
32. R. R. Sharpe, *Calendar of Wills Proved and Enrolled in the Court of Husting, London, A.D. 1258–A.D. 1688* (J. C. Francis, London, 1889).
33. S. K. Cohn, Jr., *The Black Death Transformed: Disease and Culture in Early Renaissance Europe* (Arnold, London, United Kingdom, 2003).
34. National Archives (United Kingdom), Research guides: Wills 1384–1858. http://www.nationalarchives.gov.uk/help-with-your-research/research-guides/wills-1384-1858/. Accessed 13 July 2018.
35. A. Bushby, "Demographic patterns in medieval London inferred from wills probated in the court of Husting, 1259–1689," MSc thesis, McMaster University, Hamilton, ON, Canada (2019).
36. J. Ginsberg *et al.*, Detecting influenza epidemics using search engine query data. *Nature* **457**, 1012–1015 (2009).
37. J. Roosen, D. R. Curtis, Dangers of noncritical use of historical plague data. *Emerg. Infect. Dis.* **24**, 103–110 (2018).
38. W. G. Bell, *The Great Plague in London in 1665* (John Lane; Dodd, Mead and Company OCLC, London, 1924).
39. A. A. King, M. D. de Cellès, F. M. G. Magpantay, P. Rohani, Avoidable errors in the modeling of outbreaks of emerging pathogens, with special reference to Ebola. *Proc. R. Soc. Lond. B* **282**, 20150347 (2015).
40. J. Wallinga, M. Lipsitch, How generation intervals shape the relationship between growth rates and reproductive numbers. *Proc. R. Soc. Lond. B* **274**, 599–604 (2007).
41. J. Ma, D. J. D. Earn, Generality of the final size formula for an epidemic of a newly invading infectious disease. *Bull. Math. Biol.* **68**, 679–702 (2006).

42. D. A. Rolls, P. Wang, E. McBryde , P. Pattison, G. Robins, A simulation study comparing epidemic dynamics on exponential random graph and edge-triangle configuration type contact network models. *PLoS One* **10**, e0142181 (2015).
43. J. D. Marshall, Jr, D. V. Quy, F. L. Gibson, Asymptomatic pharyngeal plague infection in Vietnam. *Am. J. Trop. Med. Hyg.* **16**, 175–177 (1967).
44. R. Gani, S. Leach, Epidemiologic determinants for modeling pneumonic plague outbreaks. *Emerg. Infect. Dis.* **10**, 608–614 (2004).
45. M. Laroche, D. Raoult, P. Parola, Insects and the transmission of bacterial agents. *Microbiol. Spectr.* **6**, MTBP-0017-2016 (2018).
46. V. Laperriére, D. Badariotti, A. Banos, J.-P. Müller, Structural validation of an individual-based model for plague epidemics simulation. *Ecol. Complex.* **6**, 102–112 (2009).
47. V. M. Dubyanskiy, A. B. Yeszhanov, "Ecology of *Yersinia pestis* and the epidemiology of plague" in *Yersinia pestis: Retrospective and Perspective*, R. Yang, A. Anisimov, Eds. (Advances in Experimental Medicine and Biology 918, Springer, 2016), pp. 101–170.
48. R. Finlay, *Population and Metropolis: The Demography of London* (Cambridge Geographical Studies, Cambridge University Press, Cambridge, 1981), vol. 12, pp. 1580–1650.
49. R. Finlay, B. Shearer, "Population growth and suburban expansion" in *London 1500–1700: The Making of the Metropolis*, A. L. Beier, R. Finlay, eds. (Longman, 1986), pp. 37–59.
50. O. Krylova, "Predicting epidemiological transitions in infectious disease dynamics: Smallpox in historic London (1664-1930)," PhD thesis, McMaster University, Hamilton, ON, Canada (2011).
51. S. Porter, *The Great Plague* (Amberley Publishing, 2009), p. 14.
52. M. McCormick, Rats, communications, and plague: Toward an ecological history. *J. Interdiscipl. Hist.* **34**, 1–25 (2003).
53. M. J. Keeling, C. A. Gilligan, Bubonic plague: A metapopulation model of a zoonosis. *Proc. R. Soc. Lond. B* **267**, 2219–2230 (2000).
54. K.-B. G. Scholthof, The disease triangle: Pathogens, the environment and society. *Nat. Rev. Microbiol.* **5**, 152–156 (2007).
55. F. E Matthes, Report of committee on glaciers, April 1939. *Eos. Trans. Am. Geophys. Union* **20**, 518–523 (1939).
56. P. D. Jones, A. E. J. Ogilvie, T. D. Davies, K. R. Briffa, *History and Climate: Memories of the Future?* (Springer Science & Business Media, 2013).
57. D. C. Cavanaugh, Specific effect of temperature upon transmission of the plague bacillus by the oriental rat flea, *Xenopsylla cheopis*. *Am. J. Trop. Med. Hyg.* **20**, 264–273 (1971).
58. L. Xu *et al.*, Nonlinear effect of climate on plague during the third pandemic in China. *Proc. Natl. Acad. Sci. U.S.A.* **108**, 10214–10219 (2011).
59. L. Xu *et al.*, Wet climate and transportation routes accelerate spread of human plague. *Proc. R. Soc. Lond. B* **281**, 20133159 (2014).
60. H. V. Pham, D. T. Dang, N. N. Tran. Minh, N. D. Nguyen, T. V. Nguyen, Correlates of environmental factors and human plague: An ecological study in Vietnam. *Int. J. Epidemiol.* **38**, 1634–1641 (2009).
61. R. P. H. Yue, H. F. Lee, Pre-industrial plague transmission is mediated by the synergistic effect of temperature and aridity index. *BMC Infect. Dis.* **18**, 134 (2018).
62. T. Ben Ari *et al.*, Interannual variability of human plague occurrence in the Western United States explained by tropical and North Pacific Ocean climate variability. *Am. J. Trop. Med. Hyg.* **83**, 624–632 (2010).
63. A. M. Schotthoefer *et al.*, Effects of temperature on the transmission of *Yersinia pestis* by the flea, *Xenopsylla cheopis*, in the late phase period. *Parasit. Vectors* **4**, 191 (2011).
64. A. Nesje, S. O. Dahl, T. Thun, Ø. Nordli, The 'Little Ice Age' glacial expansion in western Scandinavia: Summer temperature or winter precipitation? *Clim. Dynam.* **30**, 789–801 (2008).
65. S. W. Park, J. Dushoff, D. J. D. Earn, H. Poinar, B. M. Bolker, Human ectoparasite transmission of the plague during the second pandemic is only weakly supported by proposed mathematical models. *Proc. Natl. Acad. Sci. U.S.A.* **115**, E7892–E7893 (2018).
66. C. McEvedy, The bubonic plague. *Sci. Am.* **258**, 118 (1988).
67. J. L. Kool, R. A. Weinstein, Risk of person-to-person transmission of pneumonic plague. *Clin. Infect. Dis.* **40**, 1166–1172 (2005).
68. World Health Organization, International travel and health: Plague. http://www.who.int/ith/diseases/plague/en/. Accessed 12 June 2018.
69. World Health Organization, Plague: Key facts. http://www.who.int/en/news-room/fact-sheets/detail/plague. Accessed 16 June 2018.
70. R. J. Eisen *et al.*, Early-phase transmission of *Yersinia pestis* by unblocked fleas as a mechanism explaining rapidly spreading plague epizootics. *Proc. Natl. Acad. Sci. U.S.A.* **103**, 15380–15385 (2006).
71. R. J. Eisen, A. P. Wilder, S. W. Bearden, J. A. Montenieri, K. L. Gage, Early-phase transmission of *Yersinia pestis* by unblocked *Xenopsylla cheopis* (Siphonaptera: Pulicidae) is as efficient as transmission by blocked fleas. *J. Med. Entomol.* **44**, 678–682 (2007).
72. B. J. Hinnebusch, D. M. Bland, C. F. Bosio, C. O. Jarrett, Comparative ability of *Oropsylla montana* and *Xenopsylla cheopis* fleas to transmit *Yersinia pestis* by two different mechanisms. *PLoS Neglected Trop. Dis.* **11**, e0005276 (2017).
73. World Health Organization, WHO director-general's opening remarks at the media briefing on COVID-19 - 11 March 2020. https://www.who.int/dg/speeches/detail/who-director-general-s-opening-remarks-at-the-media-briefing-on-covid-19—11-march-2020. Accessed 10 June 2020.
74. G. Meyerowitz-Katz, L. Merone, A systematic review and meta-analysis of published research data on COVID-19 infection-fatality rates. medRxiv:2020.05.03.20089854 (7 July 2020).
75. A. Basu, Estimating the infection fatality rate among symptomatic COVID-19 cases in the United States. *Health Aff.* **39**, 1229–1236 (2020).
76. D. J. D. Earn, J. Dushoff, S. A. Levin, Ecology and evolution of the flu. *Trends Ecol. Evol.* **17**, 334–340 (2002).
77. N. Johnson, J. Mueller, Updating the accounts: Global mortality of the 1918-1920 "Spanish" influenza pandemic. *Bull. Hist. Med.* **76**, 105–115 (2002).
78. J. Dushoff, J. B. Plotkin, C. Viboud, D. J. D. Earn, L. Simonsen, Mortality due to influenza in the United States—An annualized regression approach using multiple-cause mortality data. *Am. J. Epidemiol.* **163**, 181–187 (2006).
79. S. W. Park *et al.*, Reconciling early-outbreak estimates of the basic reproductive number and its uncertainty: framework and applications to the novel coronavirus (SARS-CoV-2) outbreak. *J. R. Soc. Interface* **17**, 20200144 (2020).
80. S. W. Park *et al.*, Cohort-based approach to understanding the roles of generation and serial intervals in shaping epidemiological dynamics. medRxiv:2020.06.04.20122713 (5 June 2020).
81. S. W. Park, D. M. Cornforth, J. Dushoff, J. S. Weitz, The time scale of asymptomatic transmission affects estimates of epidemic potential in the COVID-19 outbreak. *Epidemics*, **31**, 100392 (2020).
82. A. Abbott, The 'time machine' reconstructing ancient Venice's social networks. *Nature* **546**, 341–344 (2017).
83. B. M. Bolker, *Ecological Models and Data in R* (Princeton University Press, 2008).
84. F. J. Richards, A flexible growth function for empirical use. *J. Exp. Bot.* **10**, 290–301 (1959).
85. M. E. Brooks *et al.*, glmmTMB balances speed and flexibility among packages for zero-inflated generalized linear mixed modeling. *R J.* **9**, 378–400 (2017).
86. C. Viboud, L. Simonsen, G. Chowell, A generalized-growth model to characterize the early ascending phase of infectious disease outbreaks. *Epidemics* **15**, 27–37 (2016).
87. G. Chowell, L. Sattenspiel, S. Bansal, C. Viboud, Mathematical models to characterize early epidemic growth: A review. *Phys. Life Rev.* **18**, 66–97 (2016).
88. D. Champredon, D. J. D. Earn, Understanding apparently non-exponential outbreaks. Comment on "mathematical models to characterize early epidemic growth: A review" by Gerardo Chowell et al. *Phys. Life Rev.* **18**, 105–108 (2016).

PNAS
www.pnas.org

Supplementary Information for

Acceleration of plague outbreaks in the second pandemic

David J. D. Earn, Junling Ma, Hendrik Poinar, Jonathan Dushoff, Benjamin M. Bolker

E-mail: earn@math.mcmaster.ca

DOI: 10.1073/pnas.2004904

This PDF file includes:

Supporting Information Text

Historical human population estimates for London

See Table S1 and Figure S1.

Disease-related data sources

Table S2 lists our data sources. Below we provide a few additional comments and details not described in the text of the main paper.

Last wills and testaments.

London 1348–1375: Cohn (1) presents his monthly counts of wills (proved by the Court of Husting, London (2)) in his Figures 7.33 (1348), 7.34 (1361) and 7.35 (1375); Cohn does not show data for 1368. Monthly aggregations of our daily counts agree nearly perfectly with Cohn's plots for the three epidemics he studied. Most of the slight discrepancies are probably attributable to a small number of wills that were written during the plague epidemics but probated much later (so not included by Cohn (1)).

London 1384–1678: The wills proved by the Prerogative Court of Canterbury (PCC) provide a substantial sample of London wills, but certainly not all the wills written by Londoners at the time, as the following quote from the National Archives website makes clear.

> "Most people who left a will used the appropriate church court. The Prerogative Court of Canterbury was the highest church court in England and Wales until 1858, when the national court was established, but even in the late 1850s it was only proving about 40% of the national total of 21,653 wills.
>
> Until 1858 there were more than 200 church courts each of which kept separate registers of wills – there was no central index.
>
> ...
>
> Wills proved in the Prerogative Court of Canterbury (PCC) mainly relate to testators resident in the south of England, although all parts of England and Wales are represented in the records."
>
> – The UK National Archives

Before the 17th century, the number of PCC wills is too small to detect an epidemic signal (see the PCC wills plotted in the top two panels of Figure S6, which we have not used for growth rate estimates). Consequently, studying potential plague epidemics in the 15th century—after the period when many London wills were probated in the Court of Husting and before many London wills were probated in the Court of Canterbury—would probably require analysis of the records of a substantial fraction of church courts. Creighton (3, Ch. IV) gives numerous historical references that indicate specific plague epidemics in London between 1375 and 1540. Unfortunately, none of these sources provides an outbreak time series, so there is no possibility of estimating epidemic growth rates.

Will dates vs. probate dates. The Calendar of Wills probated in the Court of Husting (2) is organized by court dates, so every will is associated with a definite date on which it was probated; in contrast, only 64% of the wills provide information on the date of writing (4). Despite this lower sample size and the fact that wills were in some cases written long before death, dates of writing actually provide a much more plausible representation of the epidemic patterns in the 14th century than probate dates (Figure S2). Graphs in the main text (Figures 1 to 3) are based on counts of wills written. See "Wills and testaments" in the Data section of the main text for further discussion.

London Bills of Mortality (LBoM).

London 1563–1583: The earliest weekly plague mortality records are tabulated by Creighton (3) for 1563–1564 (3, p. 305) and 1578–1583 (3, p. 341–344).

London 1593: The extant records of weekly plague mortality in London in 1593 (Figure S6, second panel) are implausible. One possibility is that many earlier deaths were added to the counts for two of the weeks in July, but there is no way to be sure. Creighton (3, pp. 351–360) discusses all the data ever found for the epidemic of plague in 1592–1593, states that the weekly data probably originate from marginal notes in a broadside of 1603, and comments (p. 354) that "the weekly mortalities in it for those weeks that had little plague are an absurdity for 1593. Whatever the source of this table, it is not genuine for 1593 ..."

London 1603–1680: Creighton (3) tabulates data for 1606–1610 (3, p. 494) and 1636 (3, p. 530). Bell (5) and Creighton (3) both tabulate weekly mortality from 1605 to the end of 1665, which includes the majority of the Great Plague in 1665–1666 (3, p. 662). We entered all weekly mortality data from 1662 to 1680 directly from the London Bills of Mortality.

Parish registers. Cummins *et al.* (6) obtained parish register data from `ancestry.com` and have made the weekly counts of deaths available at `http://neilcummins.com`. For the 16th and 17th century epidemics, the parish data provide a third source. For 1593, these are the only reliable data (we consider them to be reliable because they are part of a continuous weekly time series from 1538 onwards).

Major vs minor plague epidemics. Figure S3 shows all weekly reports of plague deaths from the LBoM from 1563 to 1666, scaled by population size (estimated by interpolating from Table S1). Epidemics with peak plague mortality above 5 per 1000 individuals per week were classified as *major*. With the exception of 1593 (for which we do not use LBoM data; see above), all these major epidemics peak above 14 on this scale; all the other (*minor*) epidemics peak below 3. The raw plague mortality data are shown in Figure S4.

We classify all the 14th century epidemics as 'major', although we do not have appropriate data to distinguish major from minor epidemics in this early epoch.

Weekly time series for all the major epidemics are shown in Figures S5 and S6.

Generation interval for bubonic plague

For pneumonic plague, sufficiently detailed data exist for a number of modern outbreaks to allow an estimate of the latent and infectious periods (and hence of the generation interval distribution) (7), which we can use to estimate $\mathcal{R}_0$ for a given value of r (8). Much less data is available for bubonic plague; in addition, the more complex host-vector life cycle of bubonic plague complicates the estimation of the generation interval. However, we can say that the elapsed time between the onset of infectiousness of a rat and the time when a rat in the next infection cycle becomes infectious is:

$$\begin{aligned} & \text{rat} \to \text{flea infection time} \\ + \;& \max\big(\text{flea incubation period}, \{\text{time to rat death} + \text{flea searching time}\}\big) \\ + \;& \text{flea} \to \text{rat infection time} \\ + \;& \text{rat incubation period} \end{aligned} \qquad [S1]$$

The second line above takes account of the fact that a flea leaves its rat host when, and only when, the rat dies (9). From (10), we can gather that

- fleas bite rats ≈ 4 times/day; the rat $\to$ flea infection probability is ≈ 0.2 and the flea $\to$ rat infection probability is ≈ 0.28, suggesting that both the rat $\to$ flea and flea $\to$ rat infection times are ≈ 1 day;
- the rat infectious period (time until infected rats die) is ≈ 4 days ((10) cite (11) for this value; (12) give a value of ≈ 18 days, which seems unrealistically long — another source, (13), gives values ranging from $\approx$ 4–9 days)
- the flea incubation period is long (but very variable), ranging from 9–26 days ((10), citing (14))
- the flea searching time is not explicitly defined by (10), but we guess it is relatively short ($<$ 1–2 days)
- (10) give a value of $\approx$ 1–3 days for the rat incubation period

Since the flea incubation period is typically longer than the combination of rat death time and flea searching time (9–26 days vs. (4–9 + 1–2) days), we can approximate the generation interval as $\approx$ (1 day) + (9–26 days) + (1 day) + (1–3 days); we use a value of $T_g = 18$ days in the main text.

Relationship between rat density and $\mathcal{R}_0$ (in rats)

One factor that might have contributed to the observed increase in epidemic growth rates in London is the density of rats. We do not have data that allow us to estimate rat densities in Medieval England, but we can ask—all else being equal—by what factor would rat density have to have changed in order to account for the observed change in growth rates?

In the idealized situation in which the generation interval is exponentially distributed (as in the standard SIR model) then (8), as mentioned in the Discussion in the main text,

$$r = \frac{\mathcal{R}_0 - 1}{T_g}\,, \qquad [S2]$$

where T_g is the mean generation interval. Consequently, if this simple relationship holds and the mean generation interval *does not change*, then a change in growth rate $r_1 \to r_2$ implies a change in basic reproduction number $\mathcal{R}_{0,1} \to \mathcal{R}_{0,2}$, where

$$\frac{\mathcal{R}_{0,2}}{\mathcal{R}_{0,1}} = \frac{r_2 T_g + 1}{r_1 T_g + 1}\,. \qquad [S3]$$

If we assume the estimate of $T_g = 18$ days obtained above, and the MLE growth rates from early and late wills listed in Table 1, the relative change in reproduction number that needs explanation is

$$\frac{\mathcal{R}_{0,2}}{\mathcal{R}_{0,1}} \approx \frac{23 \cdot \frac{18}{365} + 1}{5.86 \cdot \frac{18}{365} + 1} \approx \frac{2.13}{1.29} \approx 1.65\,. \qquad [S4]$$

where the second subscript (1 or 2) denotes the early or late epoch, respectively.

Keeling and Gilligan (12, p. 2226) relate the basic reproduction number to rat density via

$$\mathcal{R}_0 = \frac{\beta_{\mathrm{R}} K_{\mathrm{F}}}{d_{\mathrm{F}}} \left[1 - \exp\left(-aK_{\mathrm{R}}\right)\right], \qquad [S5]$$

where β and K denote transmission rate and carrying capacity, respectively, and the subscripts F and R denote fleas and rats, respectively. Equation (S5) implies

$$\frac{\mathcal{R}_{0,2}}{\mathcal{R}_{0,1}} = \frac{1 - \exp\left(-aK_{\mathrm{R},2}\right)}{1 - \exp\left(-aK_{\mathrm{R},1}\right)}, \qquad [S6]$$

which, for $aK_{\mathrm{R},j} \ll 1$, simplifies to

$$\frac{\mathcal{R}_{0,2}}{\mathcal{R}_{0,1}} \approx \frac{K_{\mathrm{R},2}}{K_{\mathrm{R},1}} \quad . \qquad [S7]$$

The approximation (appropriate in the limit $aK \to 0$) provides a lower bound to the true relationship, indicating that rat density would have had to increase by at least a factor of 1.65 to account for a similar increase [Equation (S4)] in $\mathcal{R}_0$.

Figure S7 shows the exact relationship [Equation (S6)] for several values of $aK_{\mathrm{R},1}$, together with the approximation for small aK [Equation (S7)]. Keeling and Gilligan (12, Table 1, p. 2221) adopt values of a and K_{R} that yield $aK_{\mathrm{R}} = 10$. If this is the correct order of magnitude for $aK_{\mathrm{R},1}$ then Equation (S6) implies that no increase in rat density would be sufficient to yield an increase in $\mathcal{R}_0$ by a factor of 1.65 (or any factor detectably greater than 1).

Effects of rat ecology on growth rates

In the Discussion in the main text, we listed "ecological and demographic changes" as a possible cause of acceleration of plague epidemics. Could changes in rat ecology plausibly have contributed to changes in epidemic growth rates?

As a vector-borne disease, the rate of bubonic plague spread is primarily affected by the flea-rat ratio. In the traditional Ross-MacDonald model for vector-borne epidemics, $\mathcal{R}_0$ is proportional to the square of vector-host ratio because vectors must independently bite hosts twice (once to become infected and a second time to infect a susceptible host). In the rat-flea model, $\mathcal{R}_0$ is instead proportional to V/H because *all* infected fleas on a host disperse and bite other hosts when their initial host dies. From Keeling and Gilligan's plague model (12), the expected change in r for a change in flea-rat ratio from $K_{\mathrm{F}0}$ to K_{F} is $(K_{\mathrm{F}}/K_{\mathrm{F}0})^S$, where S is the sensitivity (≈ 1.5). Thus in order to a see a fourfold increase in r we would need a change of $4^{(1/S)} \approx 2.5$, not in the rat density, but in the number of fleas per rat, which seems unlikely.

As noted in the main text, rat density has an additional, indirect effect on growth rate r and reproduction number $\mathcal{R}_0$: increasing rat density will increase the probability that fleas leaving dying rats will find new, susceptible rat hosts. To crudely estimate the magnitude of this effect, if we again consider Keeling and Gilligan's model (12) then the maximum possible effect of rat density on $\mathcal{R}_0$ by this mechanism would be proportional (if fleas have very low success in finding new rat hosts). That is, in order for $\mathcal{R}_{0,\mathrm{B}}$ to increase from ≈ 1.3 in the 14th century to ≈ 2.1 in the late epoch, rat density would have to increase by at least 62%. If fleas were already fairly successful at finding hosts in the 14th century, then changes in rat density would be expected to have only a small effect on $\mathcal{R}_0$ in rats.

Analysis of delays between wills and other sources

In order to determine the relative timing of epidemics recorded by different sources, we interpolated the parish data (which are recorded at different times from the LBoM) to find values corresponding to the LBoM dates. We quantify the relative timing in two different ways, (1) measuring the maximum cross-correlation and the lag at which this cross-correlation occurs, and (2) measuring the time difference between the epidemic peaks. As expected, the parish records are strongly correlated with LBoM (maximum correlation 0.97–0.996) and approximately synchronous (CCF lag 0–1 weeks, peak lag -0.7–1.1 weeks). The wills data are more weakly correlated (maximum correlation 0.49–0.73) and more delayed (CCF lag 3–10 weeks, peak lag 3.3–5.4 weeks).

Details of numerical optimization

Robustly fitting phenomenological epidemic curves to small, noisy data sets proved to be surprisingly challenging*. In the course of developing the full model we experimented with a range of optimizers — specifically the BFGS and Nelder-Mead options for R's `optim` function as well as R's `nlminb` function; we also tried an approach that iterated back and forth between Nelder-Mead and BFGS until convergence was achieved or the fit was sufficiently stable. We chose `nlminb` because it gave the best results (highest log likelihood) for point estimates. In general, we used the standard link functions proposed by Ma *et al.* (15), i.e., fitting most of the parameters (growth rate r, background mortality/wills rate b, final size K, Richards shape parameter s) on the log scale with a scaled-tangent link ($\eta = \tan(\pi/2 \cdot (x/2 - 1))$) for the initial condition x_0. However, we found that the scaled-tangent link declined too slowly in the tails, leading to numerical instability; we replaced it with a more standard logit link ($\eta = \log(x/(1-x))$).

With this approach we failed to achieve good (convergent) fits for only three combinations of source and outbreak year, all for minor outbreaks (London bills for 1578 and 1582, Canterbury wills for 1581); these cases are excluded from the tables and figures shown below.

*See "monsters in the basement", https://redpenblackpen.tumblr.com/post/145304820562/monsters-in-the-basement.

In the future, we would suggest that further work on reparameterization, including parameterizing the logistic by the time at which half of the final size is achieved rather than by the initial number infected, and possibly the reparameterization and regularization methods suggested by (16) for the Richards model, would be useful.

Supplementary tables cited in the main text

Tables S4 to S7.

Supplementary figure cited in the main text

Figure S8.

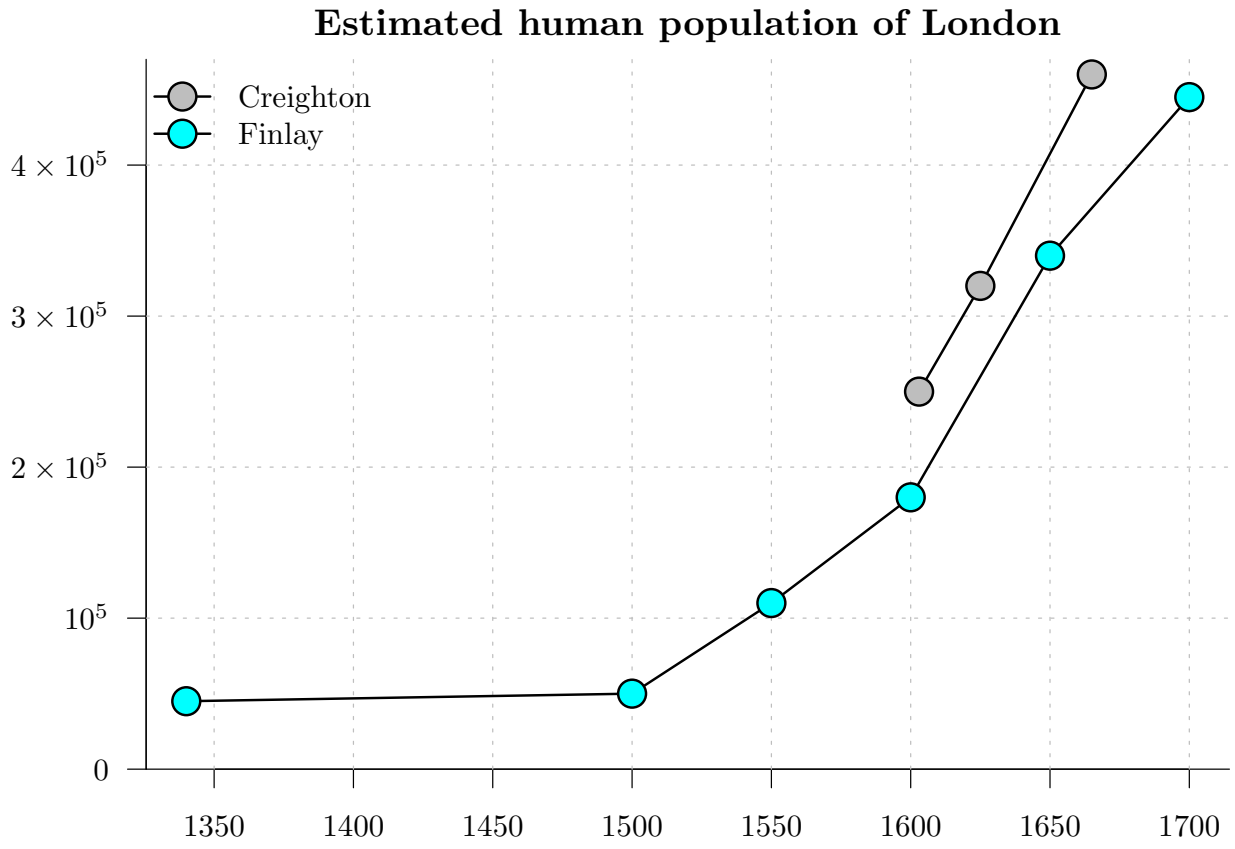

Fig. S1. Historical population of London, England, as estimated by Finlay (17, 18) (Table S1). Earlier estimates of Creighton (3, p. 660) are shown for the specific plague years 1603, 1625 and 1665.

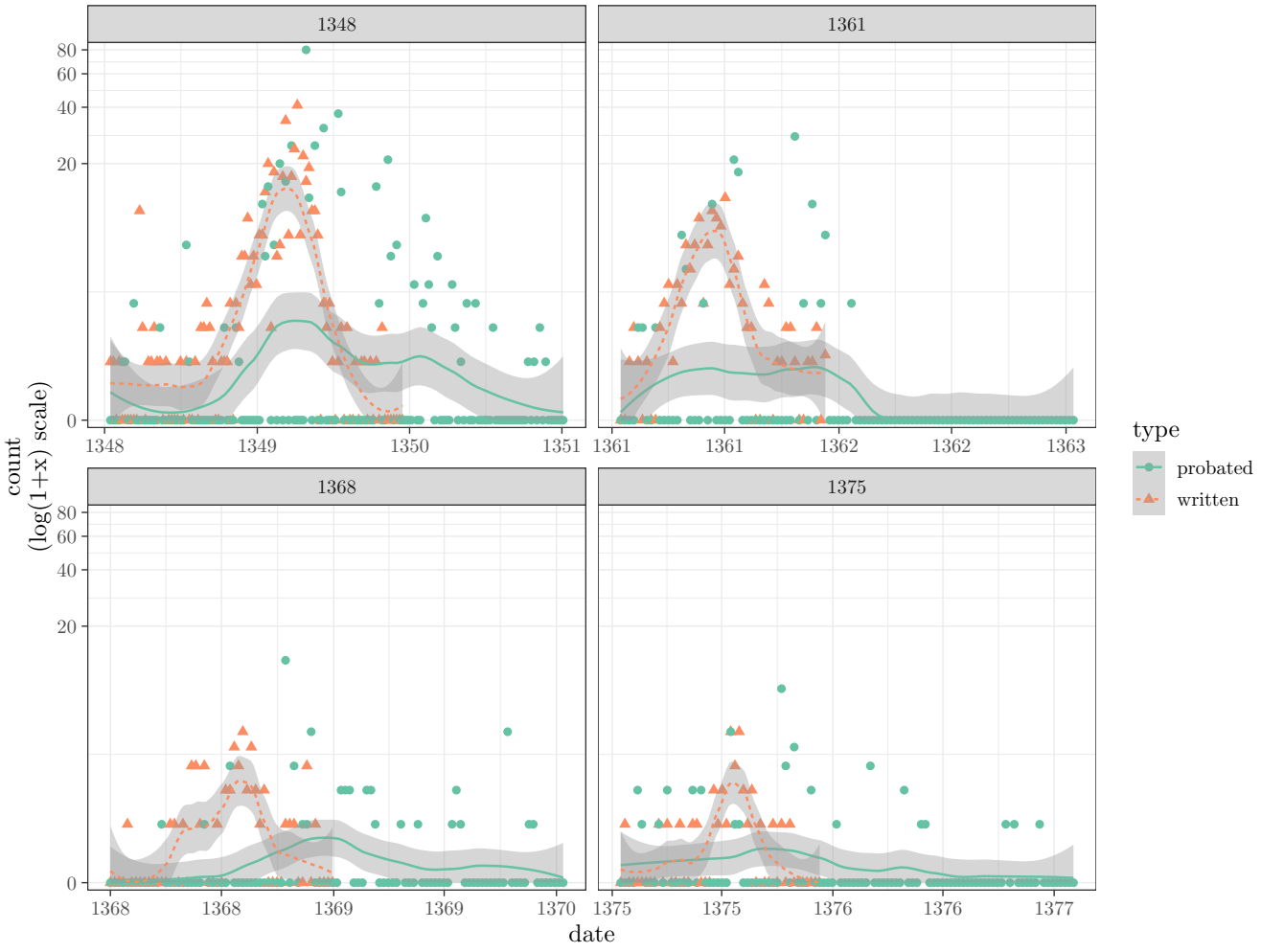

Fig. S2. Counts of wills written vs. wills probated during each of the four 14th century plague epidemics in London, based on wills probated in the Court of Husting (2). Smooth lines represent loess fits with `span=0.5` (shaded regions are 95% confidence intervals).

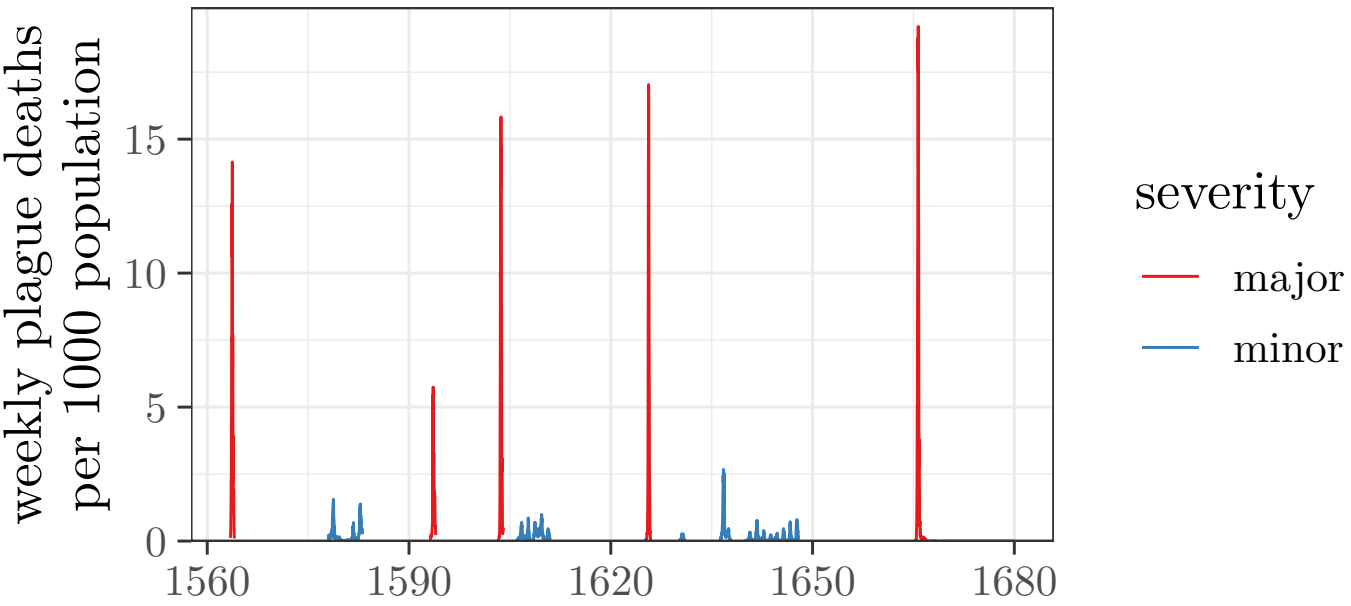

Fig. S3. Plague deaths per 1000 persons per week, from 1563 to 1666. Epidemics that exceeded 5 on this scale were classified as *major*. Analysis of the major epidemics is shown in Table 1 and Figures 2 and 3. Corresponding analyses of all of the minor epidemics are presented in Table S5 and Figure S8.

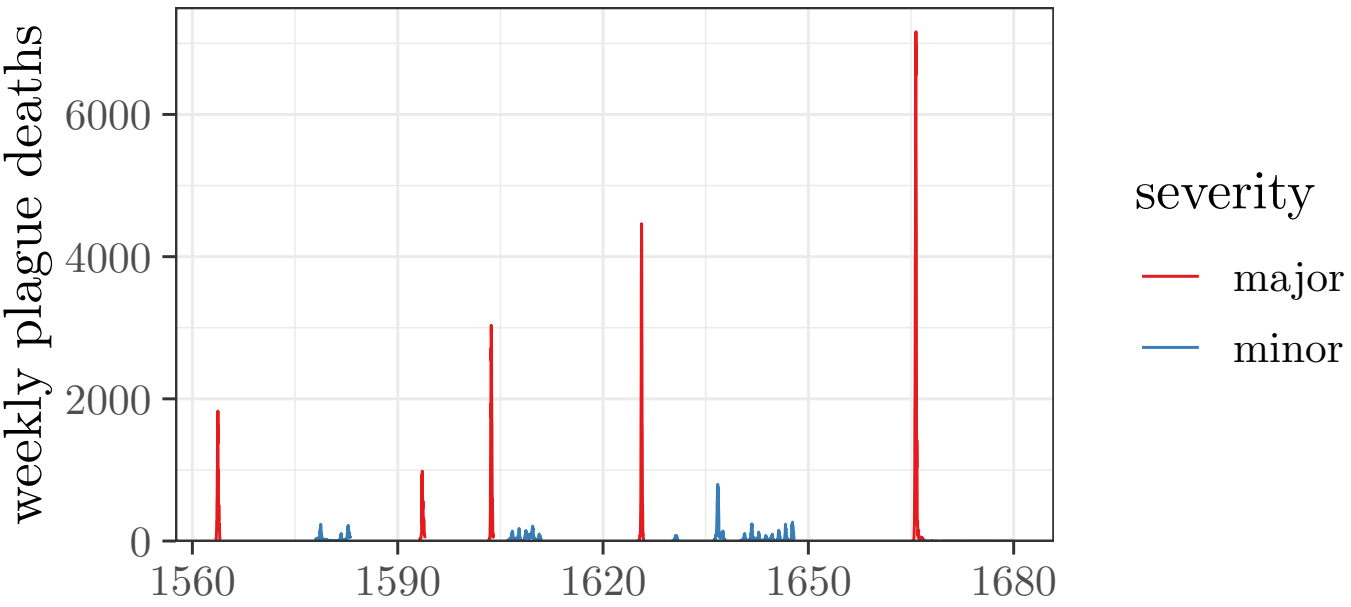

Fig. S4. All plague deaths reported in London from 1563 to 1666.

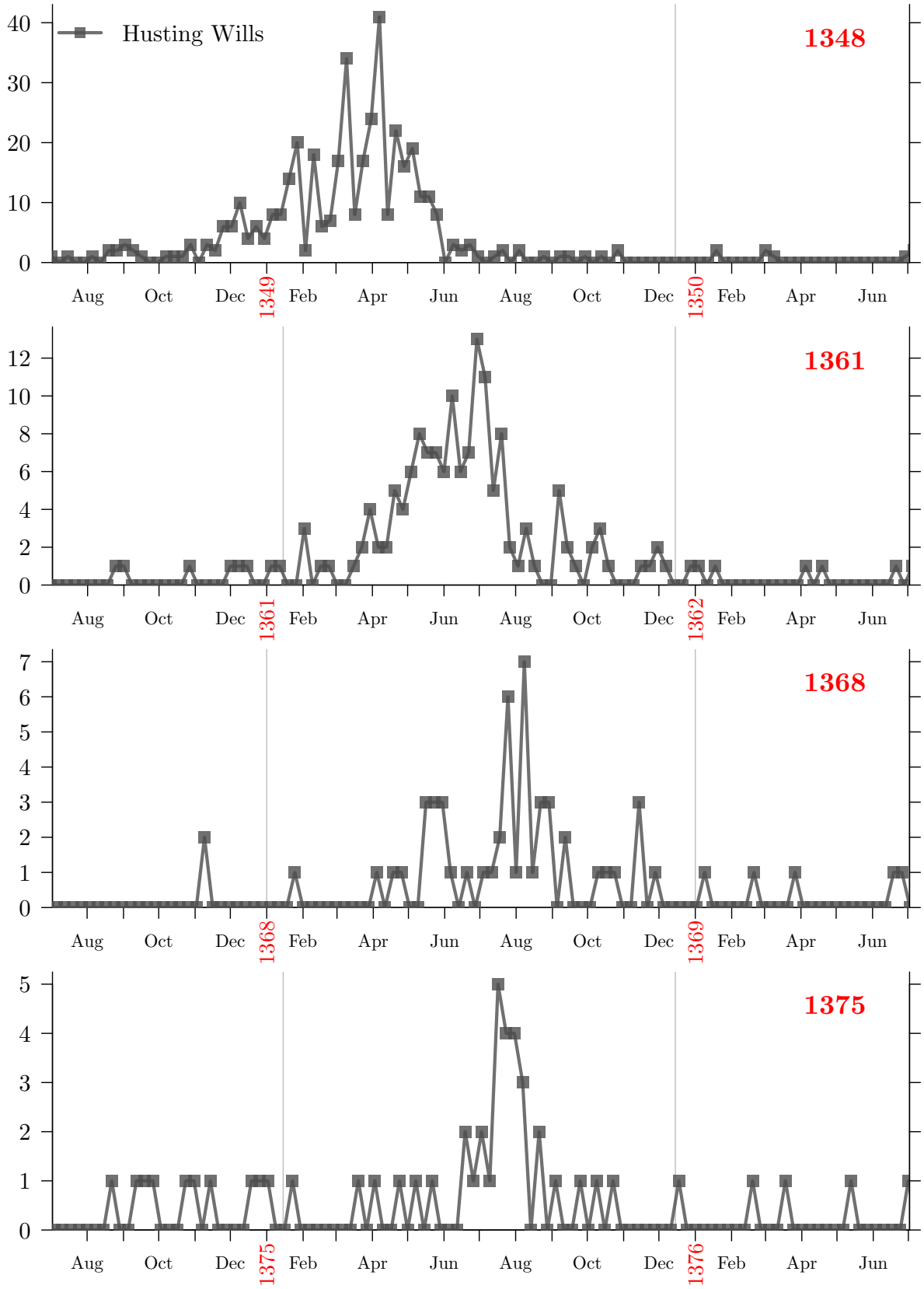

Fig. S5. Weekly numbers of wills written during plague epidemics in London, England, in the 14th century. Vertical grey lines indicate the "outbreak window" specified in Table S6.

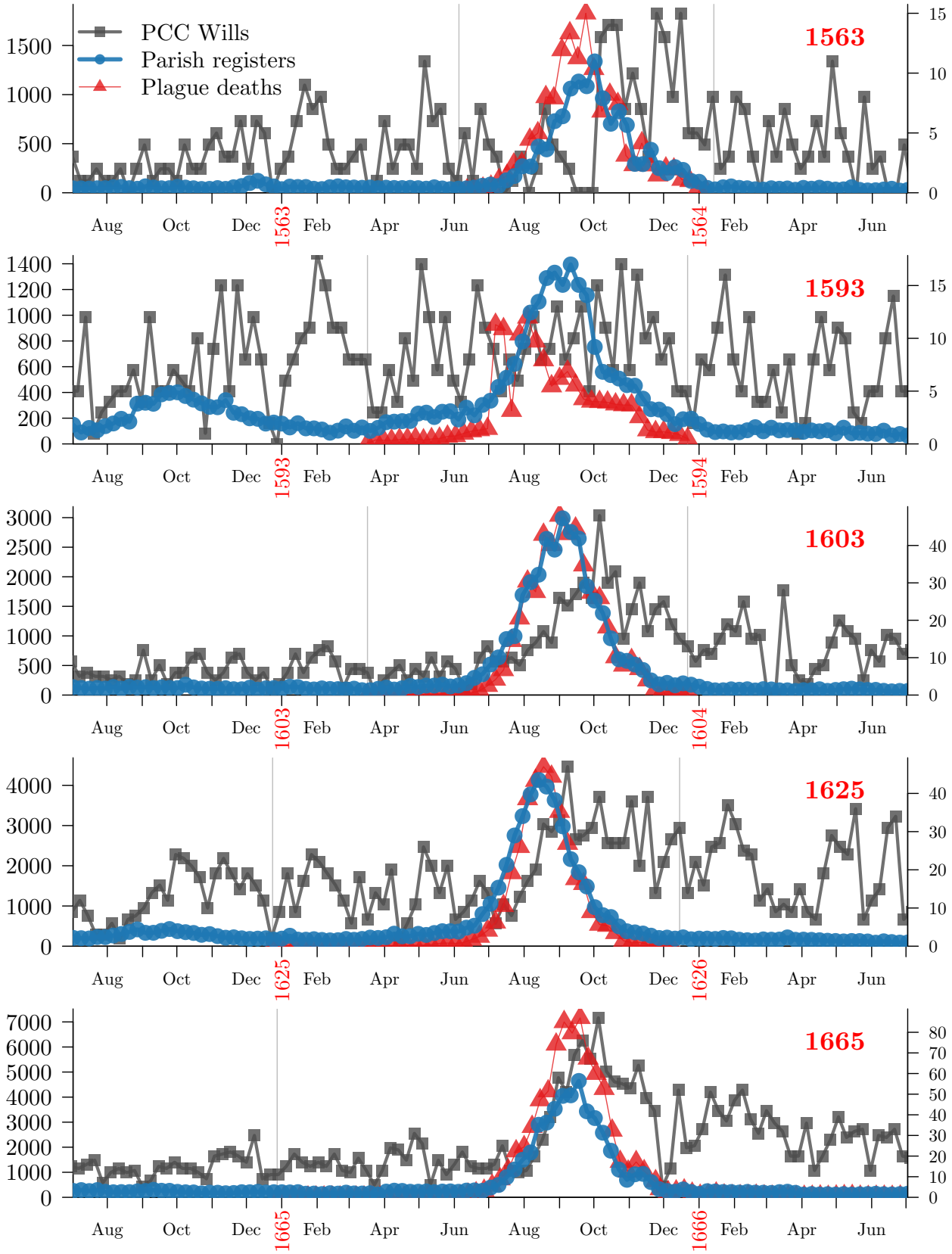

Fig. S6. Weekly deaths and numbers of wills written during major plague epidemics in London, England, since 1540. For each epidemic, vertical grey lines indicate the beginning and end of the period during which deaths from plague were listed in the bills of mortality. The left (right) scale refers to deaths (wills).

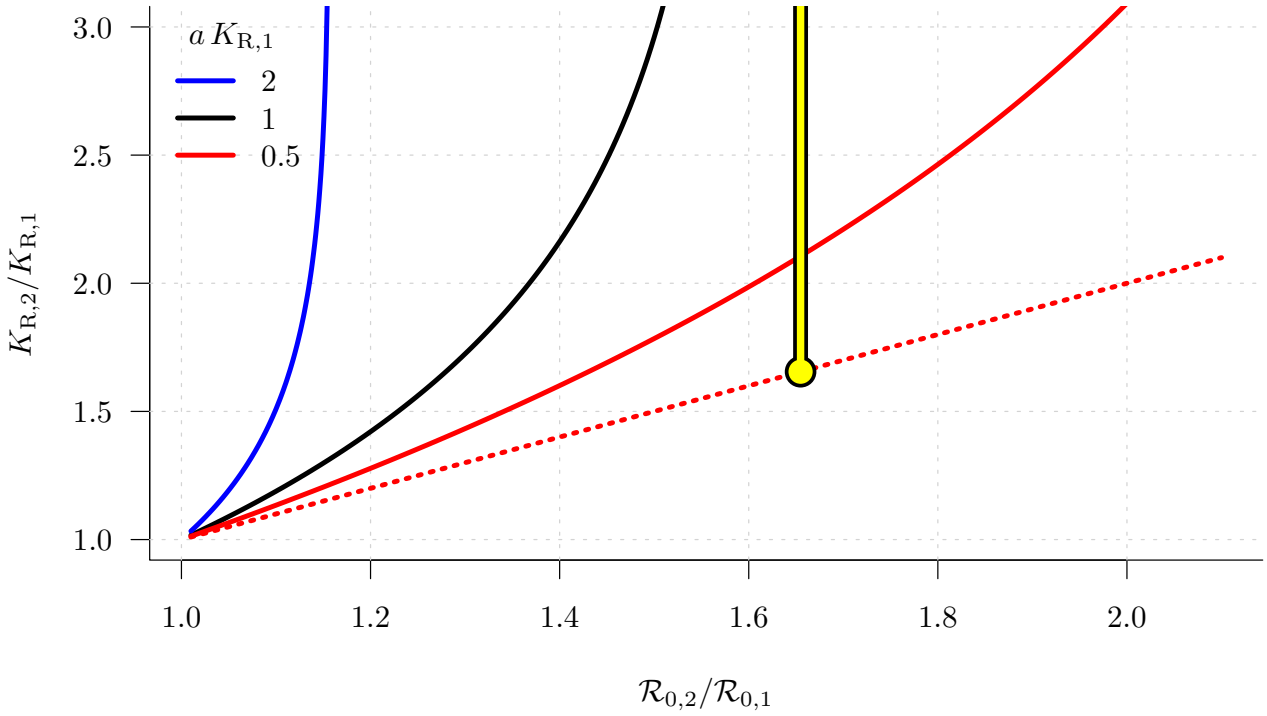

Fig. S7. Relative change in rat carrying capacity K_{R} as a function of relative change in basic reproduction number $\mathcal{R}_0$. Solid curves are based on Equation (S6). The dotted red line is based on Equation (S7). The 1.65-fold increase in $\mathcal{R}_0$ that requires explanation is indicated in yellow.

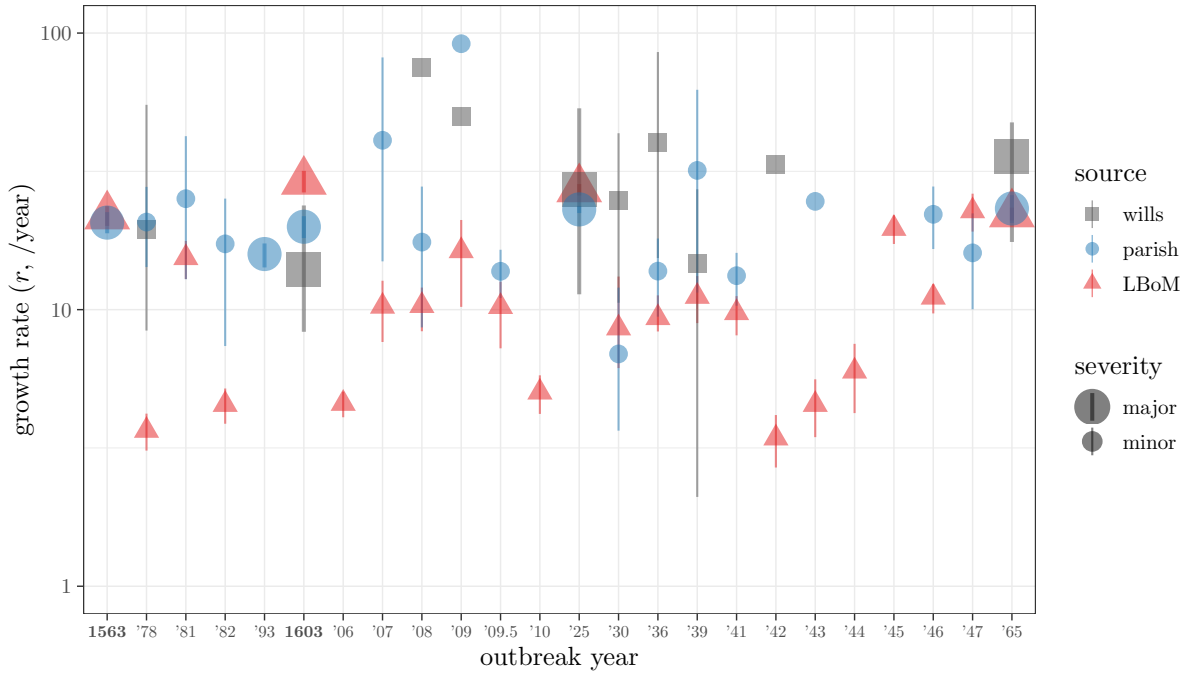

Fig. S8. Growth rate estimates for all the late epoch (1540–1680) London plague epidemics. The growth rates shown for the major epidemics are the same as those in the right panel of Figure 3. See Tables 1 and S5.

Table S1. Population estimates for London previously published by Finlay (17, 18)(19, p. 108) and Creighton (3, p. 660). These data are plotted in Figure S1.

Year	Population	Source
1340	45,000	Finlay
1500	50,000	Finlay
1550	110,000	Finlay
1600	180,000	Finlay
1603	250,000	Creighton
1625	320,000	Creighton
1650	340,000	Finlay
1665	460,000	Creighton
1700	445,000	Finlay

Table S2. Disease-related data used in this paper.

Epoch	Year range	Data type	Frequency	Source
Early	1340–1380	Last Wills and Testaments	Daily	Court of Husting
Late	1540–1680	Last Wills and Testaments	Daily	Prerogative Court of Canterbury (PCC)
	1540–1680	Mortality from all causes	Weekly	Parish records
	1563–1666	Mortality from plague	Weekly	London Bills of Mortality (LBoM)

Table S3. Observed cross-correlation and delay between London Bills of Mortality (LBoM) records and other sources. All lags measured in weeks. Rows corresponding to wills data are highlighted in grey.

source	outbreak year	CCF lag	max CCF	peak	peak lag
parish	1563	1	0.966	1563.75	1.07
parish	1603	0	0.993	1603.68	0.23
wills	1603	4	0.489	1603.78	5.45
parish	1625	0	0.986	1625.62	-0.68
wills	1625	10	0.486	1625.71	4.28
parish	1665	0	0.996	1665.70	0.15
wills	1665	3	0.726	1665.76	3.30

Table S4. Summary statistics for the model estimating differences across epochs. All parameters are in units of log(growth rate)/year. The model includes fixed effects of epoch (early [14th c.] vs. late [16th - 17th c.]) and source (wills, parish, London Bills of Mortality) and a random effect of outbreak year. Variability for each observation is assumed to be proportional to the uncertainty in its $\log(r)$ estimate (see main text, *Growth rate estimates*). In Wilkinson-Rogers notation, the model formula is: `log.r ~ epoch + source + (1|outbreak.year), disp= ~ 1+offset(log(sdvals^2))`**. Parameter estimates are given on the $\log(r)$ scale; Wald confidence intervals are given in parentheses.**

	estimate	95% CI
Intercept (14th-c. wills log growth rate)	1.768	(1.250 – 2.286)
epoch (late vs. early)	1.366	(0.517 – 2.215)
source (parish vs. wills)	-0.118	(-0.786 – 0.550)
source (LBoM vs. wills)	0.039	(-0.628 – 0.707)
nobs	16	

Table S5. Parameter estimates for minor plague epidemics (*cf.* Figure S8). Plague epidemics with $\hat{r} < 1/\mathrm{yr}$ or $\hat{r} > 100/\mathrm{yr}$, representing unreliable fits, are excluded; confidence limits that are < 0.1 or > 200 are replaced with `NA`. See *Methods* in main text.

Source	Epidemic	Growth rate [1/year]		Doubling time [days]		R^2
Wills	1578	19.4	(8.4, 55.0)	13.0	(4.6, 30.1)	0.404
LBoM	1578	3.7	(3.1, 4.2)	69.2	(60.1, 81.8)	0.825
Parish	1578	20.7	(14.3, 27.8)	12.2	(9.1, 17.7)	0.927
LBoM	1581	15.4	(12.9, 17.7)	16.4	(14.3, 19.6)	0.915
Parish	1581	25.2	(12.9, 42.4)	10.0	(6.0, 19.6)	0.784
LBoM	1582	4.5	(3.9, 5.2)	55.8	(48.8, 65.4)	0.806
Parish	1582	17.3	(7.4, 25.2)	14.6	(10.0, 34.3)	0.794
LBoM	1606	4.6	(4.1, 5.1)	55.3	(50.1, 62.0)	0.911
LBoM	1607	10.3	(7.6, 12.7)	24.6	(19.9, 33.1)	0.947
Parish	1607	41.0	(14.9, 81.6)	6.2	(3.1, 16.9)	0.757
Wills	1608	74.8	(25.8, 146.8)	3.4	(1.7, 9.8)	0.670
LBoM	1608	10.3	(8.4, 12.0)	24.5	(21.1, 30.3)	0.921
Parish	1608	17.5	(8.6, 27.9)	14.4	(9.1, 29.3)	0.728
Wills	1609	50.1	(13.0, 113.9)	5.1	(2.2, 19.5)	0.403
LBoM	1609	16.3	(10.2, 21.1)	15.5	(12.0, 24.7)	0.863
Parish	1609	91.5	(7.9, NA)	2.8	(1.1, 31.9)	0.608
LBoM	1609.5	10.2	(7.2, 12.6)	24.7	(20.1, 34.9)	0.888
Parish	1609.5	13.8	(11.0, 16.5)	18.4	(15.4, 23.0)	0.954
LBoM	1610	5.0	(4.2, 5.8)	50.3	(43.7, 60.3)	0.897
Wills	1630	24.8	(10.6, 43.4)	10.2	(5.8, 23.9)	0.415
LBoM	1630	8.6	(6.1, 13.2)	29.5	(19.2, 41.2)	0.846
Parish	1630	6.9	(3.7, 12.0)	36.6	(21.1, 69.3)	0.665
Wills	1636	40.3	(15.4, 85.4)	6.3	(3.0, 16.5)	0.663
LBoM	1636	9.3	(8.3, 11.3)	27.1	(22.5, 30.3)	0.947
Parish	1636	13.8	(9.4, 18.1)	18.4	(14.0, 26.8)	0.959
Wills	1639	14.6	(2.1, 27.2)	17.3	(9.3, 120.3)	0.063
LBoM	1639	11.2	(8.9, 13.2)	22.7	(19.1, 28.3)	0.958
Parish	1639	31.9	(11.5, 62.4)	7.9	(4.1, 21.9)	0.575
LBoM	1641	9.7	(8.1, 11.2)	26.0	(22.6, 31.3)	0.964
Parish	1641	13.3	(10.3, 16.0)	19.1	(15.8, 24.5)	0.974
Wills	1642	33.4	(6.2, NA)	7.6	(1.1, 40.5)	0.643
LBoM	1642	3.4	(2.7, 4.2)	73.8	(60.8, 94.2)	0.757
LBoM	1643	4.5	(3.5, 5.6)	55.8	(45.2, 73.1)	0.766
LBoM	1644	6.0	(4.2, 7.5)	42.3	(33.6, 59.9)	0.860
LBoM	1645	19.6	(17.3, 21.9)	12.9	(11.5, 14.6)	0.978
LBoM	1646	11.1	(9.7, 12.4)	22.8	(20.5, 26.1)	0.843
Parish	1646	22.1	(16.6, 27.9)	11.4	(9.1, 15.3)	0.946
LBoM	1647	22.7	(19.2, 26.3)	11.1	(9.6, 13.2)	0.871
Parish	1647	16.0	(10.0, 22.3)	15.8	(11.4, 25.2)	0.710

Table S6. Outbreak windows and fitting windows used in fitting the major plague epidemics. See *Methods* in main text.

		Outbreak Window		Fitting Window	
Source	Outbreak Year	start	end	start	end
Husting wills	1348	15 Jan 1348	15 Dec 1349	20 Jan 1348	13 Apr 1349
Husting wills	1361	15 Jan 1361	15 Dec 1361	04 Feb 1361	08 Jul 1361
Husting wills	1368	01 Jan 1368	01 Jan 1369	31 Jan 1368	26 Jul 1368
Husting wills	1375	15 Jan 1375	15 Dec 1375	25 Jan 1375	21 Jul 1375
London parish	1563	04 Jun 1563	15 Jan 1564	04 Jun 1563	08 Oct 1563
London bills	1563	05 Jun 1563	14 Jan 1564	19 Jun 1563	01 Oct 1563
Canterbury wills	1563	05 Jun 1563	14 Jan 1564	08 Jun 1563	14 Oct 1563
London bills	1593	17 Mar 1593	22 Dec 1593	17 Mar 1593	11 Aug 1593
Canterbury wills	1593	17 Mar 1593	22 Dec 1593	16 Jun 1593	31 Oct 1593
London parish	1593	19 Mar 1593	25 Dec 1593	11 Jun 1593	17 Sep 1593
London bills	1603	17 Mar 1603	22 Dec 1603	16 Jun 1603	08 Sep 1603
Canterbury wills	1603	17 Mar 1603	22 Dec 1603	18 Mar 1603	13 Oct 1603
London parish	1603	19 Mar 1603	25 Dec 1603	19 Mar 1603	10 Sep 1603
London bills	1625	24 Dec 1624	15 Dec 1625	02 Jun 1625	25 Aug 1625
Canterbury wills	1625	24 Dec 1624	15 Dec 1625	15 Jun 1625	14 Sep 1625
London parish	1625	25 Dec 1624	18 Dec 1625	11 Jun 1625	20 Aug 1625
London parish	1665	25 Dec 1664	18 Dec 1666	25 Dec 1664	24 Sep 1665
London bills	1665	28 Dec 1664	18 Dec 1666	13 Jun 1665	26 Sep 1665
Canterbury wills	1665	28 Dec 1664	18 Dec 1666	28 Dec 1664	27 Sep 1665

Table S7. The start and end dates for the fitting windows used in fitting the minor plague epidemics. See *Methods* in main text.

		Outbreak Window		Fitting Window	
Source	Outbreak Year	start	end	start	end
London parish	1578	25 Dec 1577	23 Apr 1581	25 Dec 1577	08 Oct 1578
London bills	1578	26 Dec 1577	20 Apr 1581	26 Dec 1577	09 Oct 1578
Canterbury wills	1578	26 Dec 1577	20 Apr 1581	07 Jan 1578	22 Nov 1578
London bills	1581	27 Apr 1581	18 Jan 1582	01 Jun 1581	05 Oct 1581
Canterbury wills	1581	27 Apr 1581	18 Jan 1582	27 Apr 1581	14 Jun 1581
London parish	1581	30 Apr 1581	15 Jan 1582	30 Apr 1581	08 Oct 1581
London parish	1582	22 Jan 1582	22 Jan 1583	22 Jan 1582	29 Oct 1582
London bills	1582	25 Jan 1582	24 Jan 1583	25 Jan 1582	25 Oct 1582
Canterbury wills	1582	25 Jan 1582	24 Jan 1583	25 Jan 1582	04 Jul 1582
London parish	1606	25 Dec 1605	04 Jun 1607	25 Dec 1605	17 Sep 1606
London bills	1606	26 Dec 1605	04 Jun 1607	26 Dec 1605	09 Oct 1606
Canterbury wills	1606	26 Dec 1605	04 Jun 1607	30 Dec 1605	21 Feb 1607
London bills	1607	11 Jun 1607	04 Feb 1608	11 Jun 1607	01 Oct 1607
Canterbury wills	1607	11 Jun 1607	04 Feb 1608	11 Jun 1607	20 Nov 1607
London parish	1607	11 Jun 1607	05 Feb 1608	11 Jun 1607	08 Oct 1607
London bills	1608	11 Feb 1608	23 Feb 1609	07 Apr 1608	07 Oct 1608
Canterbury wills	1608	11 Feb 1608	23 Feb 1609	11 Feb 1608	08 May 1608
London parish	1608	12 Feb 1608	26 Feb 1609	12 Feb 1608	24 Sep 1608
London bills	1609	02 Mar 1609	08 Jun 1609	02 Mar 1609	04 May 1609
Canterbury wills	1609	02 Mar 1609	08 Jun 1609	04 Mar 1609	28 May 1609
London parish	1609	05 Mar 1609	04 Jun 1609	05 Mar 1609	16 Apr 1609
London parish	1609.5	11 Jun 1609	26 Feb 1610	11 Jun 1609	01 Oct 1609
London bills	1609.5	15 Jun 1609	01 Mar 1610	15 Jun 1609	28 Sep 1609
Canterbury wills	1609.5	15 Jun 1609	01 Mar 1610	15 Jun 1609	07 Jul 1609
London parish	1610	05 Mar 1610	18 Dec 1610	05 Mar 1610	20 Aug 1610
London bills	1610	08 Mar 1610	20 Dec 1610	08 Mar 1610	06 Sep 1610
Canterbury wills	1610	08 Mar 1610	20 Dec 1610	08 Mar 1610	29 Jun 1610
London bills	1630	24 Dec 1629	16 Dec 1630	01 Apr 1630	05 Aug 1630
Canterbury wills	1630	24 Dec 1629	16 Dec 1630	28 Dec 1629	03 Dec 1630
London parish	1630	25 Dec 1629	18 Dec 1630	25 Dec 1629	06 Aug 1630
London bills	1636	24 Dec 1635	14 Dec 1637	05 May 1636	07 Oct 1636
Canterbury wills	1636	24 Dec 1635	14 Dec 1637	24 Dec 1635	29 May 1636
London parish	1636	25 Dec 1635	11 Dec 1637	25 Dec 1635	15 Oct 1636
London parish	1639	18 Dec 1639	05 Mar 1641	18 Dec 1639	10 Sep 1640
London bills	1639	19 Dec 1639	04 Mar 1641	23 Apr 1640	18 Sep 1640
Canterbury wills	1639	19 Dec 1639	04 Mar 1641	19 Dec 1639	03 Dec 1640
London bills	1641	11 Mar 1641	10 Mar 1642	15 Apr 1641	30 Sep 1641
Canterbury wills	1641	11 Mar 1641	10 Mar 1642	11 Mar 1641	17 Feb 1642
London parish	1641	12 Mar 1641	12 Mar 1642	12 Mar 1641	24 Sep 1641
London bills	1642	17 Mar 1642	09 Feb 1643	17 Mar 1642	06 Oct 1642
Canterbury wills	1642	17 Mar 1642	09 Feb 1643	17 Mar 1642	22 May 1642
London parish	1642	19 Mar 1642	12 Feb 1643	19 Mar 1642	01 Oct 1642
London bills	1643	16 Feb 1643	01 Mar 1644	16 Feb 1643	12 Oct 1643
London parish	1643	19 Feb 1643	04 Mar 1644	19 Feb 1643	05 Nov 1643
London parish	1644	04 Mar 1644	19 Mar 1645	04 Mar 1644	13 Aug 1644
London bills	1644	07 Mar 1644	20 Mar 1645	07 Mar 1644	11 Oct 1644
London parish	1645	26 Mar 1645	29 Jan 1646	26 Mar 1645	20 Aug 1645
London bills	1645	27 Mar 1645	29 Jan 1646	05 Jun 1645	11 Sep 1645
London bills	1646	05 Feb 1646	18 May 1647	09 Apr 1646	10 Sep 1646
London parish	1646	05 Feb 1646	21 May 1647	05 Feb 1646	03 Sep 1646
London parish	1647	21 May 1647	11 Dec 1647	21 May 1647	15 Oct 1647
London bills	1647	25 May 1647	14 Dec 1647	25 May 1647	14 Sep 1647

References

1. Cohn Jr. SK (2003) *The Black Death Transformed: Disease and Culture in Early Renaissance Europe*. (Arnold, London, United Kingdom).
2. Sharpe RR (1889) *Calendar of Wills Proved and Enrolled in the Court of Husting, London, A.D. 1258 – A.D. 1688. Preserved Among the Archives of Corporation of the City of London, at the Guildhall. Edited, with Introduction, by Reginald R. Sharpe ... Printed by Order of the Corporation of the City of London Under the Direction of the Library Committee*. (J. C. Francis).
3. Creighton C (1965) *A history of epidemics in Britain*. (Frank Cass & Co. Ltd., London and Edinburgh) Vol. 1, 2nd edition.
4. Bushby A (2019) *Demographic patterns in Medieval London inferred from wills probated in the Court of Husting, 1259–1689*. (MSc thesis, McMaster University, Canada).
5. Bell J (1665) *London's Remembrancer*. (Company of Parish Clerks).
6. Cummins N, Kelly M, Ó Gráda C (2016) Living standards and plague in London, 1560–1665. *The Economic History Review* 69(1):3–34.
7. Gani R, Leach S (2004) Epidemiologic determinants for modeling pneumonic plague outbreaks. *Emerging Infectious Diseases* 10(4):608–614.
8. Wallinga J, Lipsitch M (2007) How generation intervals shape the relationship between growth rates and reproductive numbers. Proceedings of the Royal Society of London, Series B 274:599–604.
9. Keeling MJ, Gilligan CA (2000) Metapopulation dynamics of bubonic plague. *Nature* 407:903–906.
10. Laperrière V, Badariotti D, Banos A, Müller JP (2009) Structural validation of an individual-based model for plague epidemics simulation. *Ecological Complexity* 6(2):102–112.
11. Audouin-Rouzeau F (2003) *Les chemins de la peste: Le rat, la puce et l'homme*. (Presses Universitaires de Rennes).
12. Keeling MJ, Gilligan CA (2000) Bubonic plague: a metapopulation model of a zoonosis. *Proceedings of the Royal Society of London B* 267(1458):2219–2230.
13. Tollenaere C, et al. (2010) Susceptibility to *Yersinia pestis* experimental infection in wild *Rattus rattus*, reservoir of plague in Madagascar. *EcoHealth* 7(2):242–247.
14. Pollitzer R (1952) Plague Studies: 7. Insect Vectors. *Bulletin of the World Health Organization* 7:231–242.
15. Ma J, Dushoff J, Bolker BM, Earn DJD (2014) Estimating initial epidemic growth rates. *Bulletin of Mathematical Biology* 76(1):245–260.
16. Smirnova A, Chowell G (2017) A primer on stable parameter estimation and forecasting in epidemiology by a problem-oriented regularized least squares algorithm. *Infectious Disease Modelling* 2(2):268–275.
17. Finlay R (1981) *Population and metropolis: the demography of London, 1580-1650*, Cambridge Geographical Studies. (Cambridge University Press, Cambridge) Vol. 12.
18. Finlay R, Shearer B (1986) Population growth and suburban expansion in *London 1500-1700: The Making of the Metropolis*, eds. Finlay R, Beier A. (Longman Group Limited), pp. 37–59.
19. Krylova O (2011) *Predicting epidemiological transitions in infectious disease dynamics: Smallpox in historic London (1664-1930)*. (PhD thesis, McMaster University, Canada).